New Results on Element 111 and 112

S. Hofmann, F.P. Heßberger, D. Ackermann, B. Kindler, J. Kojouharova, B. Lommel,
R. Mann, G. Münzenberg, S. Reshitko, H.J. Schött, GSI Darmstadt
A.G. Popeko, A.V. Yeremin, JINR Dubna
S. Antalic, P. Cagarda, S. Śaro, University Bratislava
H. Kettunen, M. Leino, J. Uusitalo, University Jyväskylä

The elements 110, 111, and 112 were first identified in a series of experiments in 1994 and 1996 at the SHIP velocity filter [1]. A total of 4 decay chains was measured of the isotope ^{269}110 and 9 decay chains of ^{271}110. Cross-sections of 3.5 and 15 pb, respectively, were determined. The cross-sections for element 111 and 112 were 3.5 and 1.0 pb, deduced from a total of 3 and 2 decay chains.

The new isotopes were identified by position and time correlation analysis. The data were obtained by using position-sensitive Si detectors (details of the experimental set-up and the analysis procedure are given elsewhere [2]). In order to prepare a safe identification of the ^{269}110 nucleus, the decay chain of the daughter ^{265}Hs and its excitation function were measured in a preceding irradiation. In the case of the isotope ^{271}110, the granddaughter ^{263}Sg was known from literature. Therefore the identification of these nuclei was straightforward and without a doubt. The discovery of element 110 by this work was recognized recently by a IUPAC/IUPAP Joint Working Party (JWP) [3].

Concerning the discovery of elements 111 and 112, the JWP concluded that further experiments are needed in order to fulfill the previously worked out criteria for assigning priority of discovery for these elements.

In order to confirm our previous results, we performed two experiments in 2000 aiming at new data on the synthesis and the decay pattern of ^{272}111 and ^{277}112. The irradiation took place from October 16 – 29 and May 3 – 29, respectively. The reactions were the same as in our first experiments, ^{64}Ni + ^{209}Bi → ^{273}111* and ^{70}Zn + ^{208}Pb → ^{278}112*. First results from the Z = 112 experiment were already published in [2]. Subsequent to the irradiation of ^{209}Bi with ^{64}Ni we irradiated a ^{207}Pb target aiming at the synthesis of the even-even nucleus ^{270}110. The results are presented in a succeeding contribution to this report.

In completion of the set-up used in our previous experiments, an electronic circuit was installed in the Z = 111 run, which allowed for switching off the beam within 50 μs after an implanted residue was detected by coincidence of energy and time-of-flight signal. In a subsequent time window of 10 ms a preset number of α particles (in this experiment one) was counted which then prolonged the beam-off period up to the expected measurable end of the decay chain. In our experiment 10 min were chosen, thus making provision for the detection of a possible α decay of ^{252}Md, $T_{1/2}$ = 2.3 min. This improvement considerably reduced the background and allowed for the safe detection of signals from long lived decays. The circuit was prepared already in May for the Z = 112 experiment, however, the trigger conditions could not be set properly, mainly due to the energy shift by degrader foils used in front of the
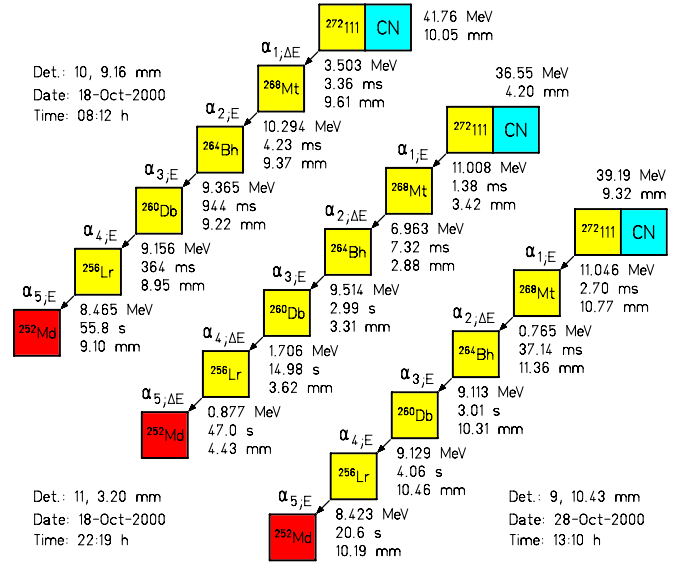

Figure 1: Decay chains and decay data measured during an experiment aiming at the confirmation of element 111.

detector.

The targets were prepared in the usual way, 450 μg/cm^2 lead or bismuth was evaporated on a 40 μg/cm^2 carbon foil. The targets were then covered by 10 μg/cm^2 carbon to protect the targets from sputtering and to improve radiative cooling.

The beam energy in the Z = 111 experiment was 320.0 MeV, the resulting excitation energy of the compound nucleus was 14.1 MeV using the mass tables of ref. [4]. At this energy we had measured 2 events in the first experiment during an irradiation time of 5.9 days (one chain was observed at 12.7 MeV excitation energy). A beam dose of 1.1×10^{18} had been collected from which a cross-section of $(3.5\ ^{+4.6}_{-2.3})$ pb resulted. In the new experiment the irradiation time was 13 days and the beam dose 2.2×10^{18} ions. A total of 3 decay chains was measured from which, in agreement with the first result, a cross-section of $(2.5\ ^{+2.5}_{-1.4})$ pb follows. The mean value from both experiments (5 events at 3.3×10^{18} projectiles) is $(2.9\ ^{+1.9}_{-1.3})$ pb.

The decay data of the 3 chains measured in the October 2000 experiment are plotted in Fig. 1. A comparison with the 3 previously measured chains and with literature data is shown in Fig. 2. The most important results are summarized in the following: 1) The trigger for the switching off the beam worked properly. All three chains were measured in full length during beam-off periods. 2) In the case of two of the three new chains (chain 5 and 6) the full α energy was measured from the decay of ^{272}111. The two energy values agree, however, the mean value of 11.03
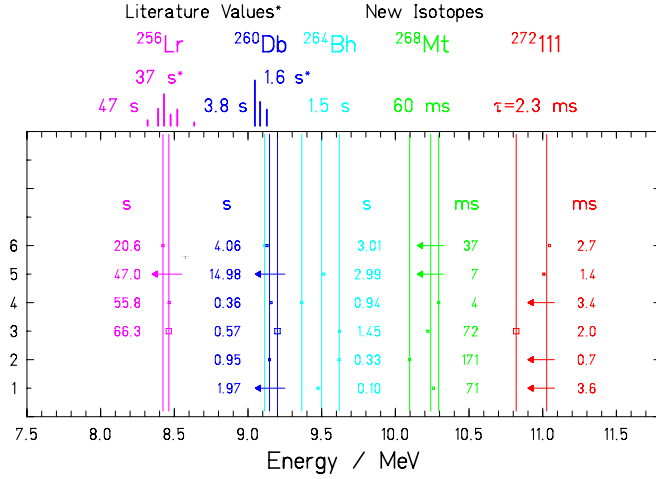
Figure 2: Comparison of α-decay data from the six events which were assigned to the decay of $^{272}111$. The event chains are chronologically ordered and numbered from 1 to 6. The size of the data points reflects the detector resolution, small dots stand for $\alpha's$ stopped in the main detector, larger squares for escape $\alpha's$ stopped in the back detectors and arrows for escape $\alpha's$ delivering only a ΔE signal from the main detector. Vertical lines are drawn at energies of single data points or at the mean energy values of transitions which have the same energy within the detector resolution. The single and mean values of lifetimes (not half-lives) are also given. Above the upper abscissa the α spectra deduced from literature are plotted for the decays of ^{256}Lr and ^{260}Db.

MeV is 0.21 MeV higher than the energy obtained from chain 3 of the first experiment. 3) The energies of the α decay of the daughter, ^{268}Mt, and granddaughter, ^{264}Bh, are spread across a wide energy range. Similar, even wider energy distributions were measured from the decay of the neighboring odd-odd isotopes ^{266}Mt and ^{262}Bh [5]. 4) A total of four α-energies was measured from the ^{260}Db decay. Three of them agree within the detector resolution. The mean value of 9.14 MeV also agrees with one of the 3 lines given in the literature. For this line energies of 9.14 and 9.12 MeV were reported [6, 7]. A slightly different, 60 keV higher energy was measured from chain 3. However, the energy value of 9.20 MeV was determined from an escape event stopped in the back detectors. For such events the energy resolution is only 40 keV (FWHM). 5) Six α lines in the energy range from 8.30 to 8.65 MeV are known from the decay of ^{256}Lr [6, 7]. Our energies from chain 3, 4, and 6 agree with the literature values. 6) The measured lifetimes agree for each of the nuclei and in the case of ^{260}Db and ^{256}Lr also with the literature values. There is only one exception. The decays of ^{268}Mt are spread across a larger lifetime period. Although the distribution is still in agreement with statistical fluctuations, it could also be possible that the longest (171 ms) or shortest (4 and 7 ms) lifetimes are related to decays from isomeric states.

Our conclusion of the recent Z = 111 experiment is that our first results are confirmed and that the new data reveal considerably improved information on the decay pattern of the chains starting at $^{272}111$.
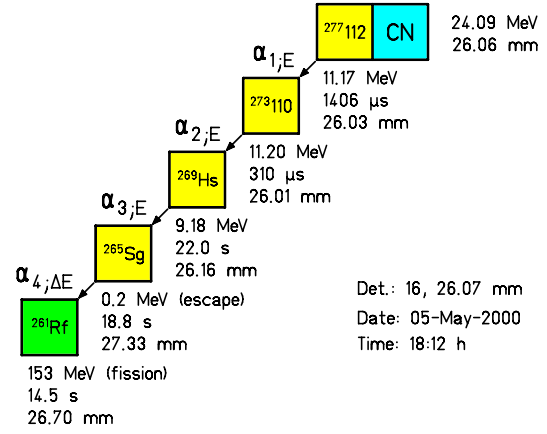

Figure 3: Decay chain of $^{277}112$ measured during a recent experiment aiming to confirm element 112.

In the study of the reaction for the synthesis of element 112 we used a beam energy of 346.1 MeV. The resulting excitation energy of 12.0 MeV is 2.0 MeV higher than in our first experiment. During an irradiation time of 19 days we collected a total of 3.5×10^{18} projectiles. One decay chain was observed. The measured data and our assignment are given in Fig. 3. The first two α decays have energies of 11.17 and 11.20 MeV, respectively, which are succeeded by an α of only 9.18 MeV, an energy step by about 2 MeV. Correspondingly, the lifetime increases by about five orders of magnitude between the second and third α decay. This decay pattern is in agreement with the one observed for chain 2 in our first experiment. It was explained as the result of a local minimum of the shell correction energy at neutron number N = 162 which is crossed by the α decay of $^{273}110$.

The α energy of 9.18 MeV for the decay of ^{269}Hs is identical within the detector resolution with the value of 9.17 MeV obtained in chain 1 of our previous experiment. A new result is the occurrence of fission ending the chain at ^{261}Rf. Fission was not yet known from ^{261}Rf, but is likely to occur taking into account the high fission probabilities of the neighboring even isotopes.

A cross-section of $(0.5^{+1.1}_{-0.4})$ pb was measured for the new data point at 12.0 MeV excitation energy. This value fits well into the systematics of cross-sections. A cross-section increase with increasing beam energy as predicted by theoretical investigation [8] was not observed.

References

[1] Hofmann, S. et al., Z. Phys. A350 (1995) 277 and 281; Z. Phys. A354 (1996) 229

[2] Hofmann, S. and Münzenberg, G., Rev. Mod. Phys. 72 (2000) 733

[3] IUPAC/IUPAP, private communication (Jan. 2001)

[4] Myers, W.D. and Swiatecki, W.J., Nucl. Phys., A601(1996) 141

[5] Hofmann, S., et al., Z. Phys. A358 (1997) 377

[6] Ghiorso, A. et al., Phys. Rev. Lett. 24 (1970) 1498

[7] Bemis, C.E. et al., Phys. Rev. C16 (1977) 1146

[8] Denisov, V.Yu. and Hofmann, S., Phys. Rev. C61 (2000) 034606

The New Isotope ^{270}110 and its Decay Products ^{266}Hs and ^{262}Sg

S. Hofmann, F.P. Heßberger, D. Ackermann, B. Kindler, J. Kojouharova,
B. Lommel, R. Mann, G. Münzenberg, H.J. Schött, GSI Darmstadt
A.G. Popeko, A.V. Yeremin, JINR Dubna
S. Antalic, P. Cagarda, S. Śaro, University Bratislava
S. Ćwiok, University Warsaw

Synthesis and investigation of heavy even-even nuclei provide especially clear data for comparison with theoretical predictions. The absence of unpaired nucleons results in unhindered α decay or spontaneous fission. Also the low-energy level scheme is expected to be relatively simple. However, the synthesis of even-even nuclei is more difficult by the fact, that in fusion reactions with ^{208}Pb and neutron rich projectiles 2 neutrons must be evaporated, or the target must be replaced by ^{207}Pb. In both cases the measured cross-sections for the synthesis of nuclei beyond rutherfordium revealed a stronger decrease than in 1n reactions using ^{208}Pb targets. Consequently, only few even-even nuclei are known beyond rutherfordium with ^{264}Hs being so far the heaviest one produced in reactions with ^{207}Pb targets [1]. Evidence of heavier even-even nuclei (^{262}116) was obtained from recent work in Dubna [2]. In this work we present results obtained in an experiment at the GSI SHIP aiming at the synthesis of the even-even nucleus ^{270}110 using the reaction ^{64}Ni + ^{207}Pb. A more detailed discussion of the results will be published in [3].
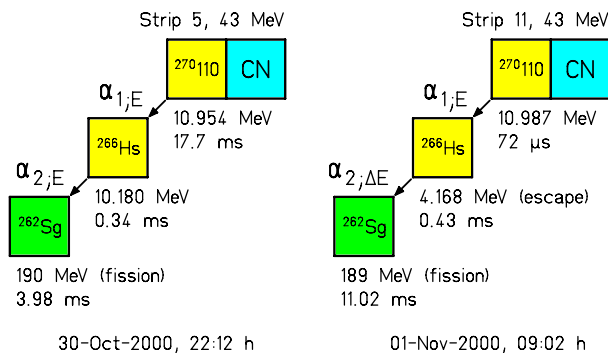

Figure 1: Two representative decay chains observed in irradiation of a ^{207}Pb target with ^{64}Ni projectiles. The chain on the left side starts with a relatively long lived α decay of ^{270}110 which is attributed to a high spin K isomer. The chain on the right side represents the decay of the short lived ground-state.

A total of eight α-decay chains was measured during an irradiation time of seven days. Two representative chains are plotted in Fig. 1. The ground-state of ^{270}110 decays by α emission with an energy of 11.03 MeV and a half-life of 100 μs. In addition we measured an isomeric level in ^{270}110 which decays with a half-life of 6.0 ms. Alpha rays with energies of 10.95, 11.15, and 12.15 MeV were attributed to the decay of the isomer. A tentative assignment of the 12.15-MeV α particle to a transition into the ground-state of ^{266}Hs results in an energy of the isomer at 1.13 MeV. The spin of the isomer was estimated from retardation of the α-decay probability to be approximately (10 ± 2) $\hbar$. A γ/IC branching of $\approx$30 % to the ground-state seems possible, but could not be definitely established.

The decay properties of the ground-state of ^{270}110 are in agreement with predictions of the macroscopic-microscopic model and with self-consistent Hartree-Fock-Bogoliubov calculations with Skyrme-Sly4 interaction. The HFB calculations resulted also in two quasiparticle excited levels, one of them could be the origin of the isomeric state. Their configuration and energy is $\{\nu[613]_{7/2+} \nu[725]_{11/2-}\}_{9-}$ at 1.31 MeV and $\{\nu[615]_{9/2+} \nu[725]_{11/2-}\}_{10-}$ at 1.34 MeV.

The new nuclei ^{266}Hs and ^{262}Sg were identified as members of the α-decay chain. The nucleus ^{266}Hs decays by α emission with an energy of 10.18 MeV and a half-life of 2.3 ms. However, it is also possible as indicated by the decay data, that the α decay has two components with half-lives of 0.35 and 6.3 ms. In that case an isomeric level would exist also in ^{266}Hs which could originate from states analogue as in the case of ^{270}110. Their energies in ^{266}Hs are predicted to be at 0.90 and 0.94 MeV using HFB calculations. For both nuclei fission was not observed. Using calculated fission half-lives, we estimated fission branchings of 0.2 and 1.4 % for the nuclei ^{270}110 and ^{266}Hs, respectively.

The nucleus ^{262}Sg decays by fission with a half-life of 6.9 ms and a total kinetic energy of the fission fragments of 222 MeV. Alpha decay was not measured, an upper limit for the α branching is 22 %. This value is in agreement with an estimate of 15 % α-branching, using a half-life deduced from a calculated value for the α energy of ^{262}Sg.

The measured cross-section of 13 pb was unexpectedly high. It is shared equally between ground-state and isomeric state.

Future experiments at longer irradiation time and higher beam dose will certainly provide a more detailed decay scheme and low-energy level scheme of ^{270}110 and its daughter nuclei. Coincidence experiments using large Ge detectors are promising to search for transitions within the rotational band in ^{266}Hs after α decay of ^{270m}110. The low-energy rotational levels can be studied via fine structure of the α decay. The measurement of the excitation function will provide data on the population of ground-state and isomeric state. The daughter nucleus ^{266}Hs could possibly be studied directly using the radiative capture reaction of ^{58}Fe and ^{208}Pb. An important next step using ^{207}Pb target is the investigation of ^{276}112. The result will demonstrate if the synthesis of even-even nuclei in cold fusion reactions could be applied also for still heavier systems.

References

[1] G. Münzenberg et al., Z. Phys. A **328** (1987) 49

[2] Yu.Ts. Oganessian et al., PR C63 (2000) 011301

[3] Hofmann, S. et al., EPJ A, to be published (2001)

Fine Structure in the α - decay of ^{255}Rf

F.P.Heßberger[1], S. Hofmann[1], D.Ackermann[1,2], A. Lavrentev[3], M. Leino[4], G. Münzenberg[1], V.Ninov[1,5], A.G. Popeko[3], S. Saro[6], Ch. Stodel[1,7], A.V.Yeremin[3]

[1]GSI, Darmstadt, Germany, [2] also Johannes Gutenberg - Universität, Mainz, Germany, [3]FLNR JINR, Dubna, Russia, [4]University of Jyväskylä, Jyväskylä, Finland, [5]now at LBNL, Berkeley, USA, [6]Comenius University, Bratislava, Slovakia, [7]now at GANIL Caen, France

In a recent experiment ^{255}Rf was produced by the reactions ^{208}Pb(^{50}Ti,3n)^{255}Rf and ^{206}Pb(^{50}Ti,n)^{255}Rf. From an unusual low number of ^{255}Rf α-decays in the energy interval (8720-8730) keV followed by α - decays of ^{251}No, the existence of a low lying isomeric state with $T_{1/2} \approx 0.9$ s was suspected [1]. Since neither from theoretical predictions [2] nor from the known levels of the lighter N=151 isotones with even Z number [3], which have a similar nuclear structure, the existence of such an isomer could be expected, we decided to clarify this problem using the reaction ^{207}Pb(^{50}Ti,2n)^{255}Rf, for which a cross section σ ≈ 10 nb was obtained. The result is shown in fig. 1a,b. On the basis of a twenty times higher number of observed counts, no ‚abnormally' low correlation rate for E_α = (8720-8730) keV was evident.
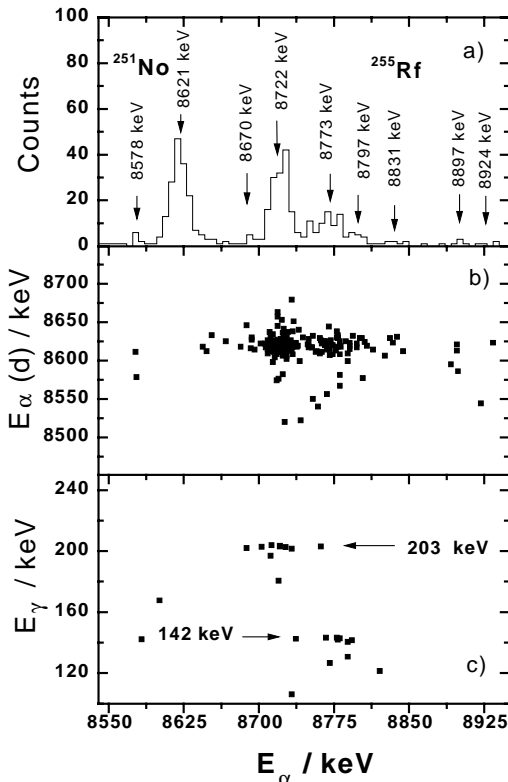

Fig. 1 Decay spectra of ^{255}Rf; a) spectrum of α - events following the implantation of a heavy residue within Δt = 20 s; b) α-α- correlation plot for ^{255}Rf → ^{251}No; c) α-γ - coincidences attributed to the decay of ^{255}Rf

In addition a few γ - events in coincidence to the α - decays of ^{255}Rf were observed (fig. 1c). Two different groups are indicated: a) γ - events of E_γ = (203±3) keV and α - decays of E_α = (8722±10) keV; b) γ - events of E_γ = (142±3) keV and E_α

= (8773±10) keV. Since for a) the sum $E_\alpha + E_\gamma$ = 8924 keV, i.e. close to the transition with the highest energy correlated to ^{251}No, we conclude that this γ - transition leads to the ground state and due to the lowest hindrance factor of HF = 3 the 8722 keV - transition is assigned to the favored transition.

According to calculations of Cwiok et al. [2] and assignments for lighter N=151 and N=149 isotones, we tentatively set the ground - states of ^{255}Rf as 9/2$^-$[734] and ^{251}No as 7/2$^+$[624] (fig. 2). Due to the striking low hindrance factor HF = 7 the 8773 keV transition cannot be assigned to the decay into the level 5/2$^+$[622], which is the first excited Nilsson level in the lighter N = 149 isotones (^{247}Cf, ^{245}Cm, ^{243}Pu) [3], although theory predicts it above the 9/2$^-$[734]. Relative intensities of decays into this level are typically lower than 0.05. Therefore we interpret the 142 keV - line due to the transition 9/2$^-$[734] → 9/2$^+$, the first member of the ground state rotational band of ^{251}No (see fig. 2). The succeeding transition 9/2$^+$ → 7/2$^+$[624] is preferrably M1 and thus highly converted. So the 8773 keV - line is understood as due to energy summing of 8722 keV - α-particles with conversion electrons. So are the α - lines at 8797 keV and 8831 keV. In theses cases we assume that primarily the 11/2$^+$ state is populated by the decay of the 9/2$^-$[734] level. The 8897 keV-line finally is understood as due energy summing between α-particles and electrons from conversion processes 9/2$^-$[734] → 7/2$^+$[624], while the small shoulder at 8670 keV may be explained by transitions into the 11/2$^-$ - state.
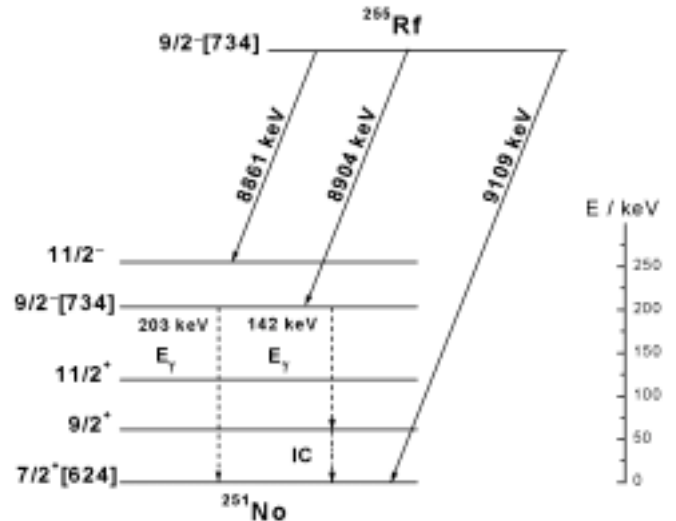

Fig. 2: Decay scheme suggested for ^{255}Rf; the energies denote the Q_α - values.

References:
[1] F.P. Heßberger et al. Z. Phys. A 359, 415 (1997)
[2] S. Cwiok et al. Nucl. Phys. A575, 356 (1994)
[3] R. Firestone et al. (eds.) Table of Isotopes (1996)

Beta Decay of ^{56}Cu

R. Borcea[1], J. Äystö[2], E. Caurier[3], P. Dendooven[2], J. Döring[1], M. Gierlik[4], M. Górska[1], H. Grawe[1], M. Hellström[1], Z. Janas[4], A. Jokinen[2], M. Karny[4], R. Kirchner[1], M. La Commara[1], K. Langanke[5], G. Martínez-Pinedo[5,6], P. Mayet[1], A. Nieminen[2], F. Nowacki[7], H. Penttilä[2], A. Płochocki[4], M. Rejmund[1], E. Roeckl[1], C. Schlegel[1], K. Schmidt[1], R. Schwengner[8], and M. Sawicka[4]

[1]*GSI, Darmstadt,* [2]*University of Jyväskylä, Finland,* [3]*Institut de Recherches Subatomiques, Strasbourg, France,* [4]*Institute of Experimental Physics, University of Warsaw, Poland,* [5]*Institut for Fysik og Astronomi, Århus Universitet Denmark,* [6]*Department für Physik und Astronomie, Universität Basel, Switzerland,* [7]*Laboratoire de Physique Théorique de Strasbourg, France,* [8]*Forschungszentrum Rossendorf e.V., Germany*

Beta-decay studies of proton-rich isotopes near the doubly closed-shell nucleus ^{56}Ni are of interest as (i) nuclei with a few nucleons outside a doubly-magic core are expected to represent comparatively simple configurations and thus be useful for testing nuclear shell-model predictions, and (ii) the large decay-energy window permits to experimentally access a sizeable fraction of the strength of the allowed β decay. Moreover, nuclear structure properties of proton-rich N $\sim$ Z isotopes are of astrophysical interest, e.g., concerning the EC cooling of supernovae and the astrophysical rp-process.

The β decay of ^{56}Cu was studied at the GSI On-line Mass Separator by using a 5.5 MeV/u ^{32}S beam from the UNILAC to induce ^{28}Si(^{32}S, p3n)^{56}Cu fusion-evaporation reactions. The reaction products were stopped in a catcher inside an ion source, released as singly-charged ions, accelerated to 55 kV and mass-separated in a magnetic field. The A=56 beam was implanted into a movable tape and investigated by means of a β-γ-γ detector array consisting of two composite high-resolution germanium (Ge) detectors and a plastic scintillator.

The ^{56}Cu decay to the doubly-magic nucleus ^{56}Ni has been investigated for the first time at the On-line Mass Separator in 1996 [1]. Four γ transitions have been observed, corresponding to the β-feedings of three excited ^{56}Ni states, and a half-life of (78 $\pm$ 15) ms has been determined. In the present experiment [2], due to the more efficient detection set-up and a longer measurement time, the quality of the data was considerably improved, and it was in particular possible to observe γ-γ coincidences. Six γ transitions were identified besides the four ones already known, three new states were added to the level scheme of ^{56}Ni, and the half-life ((92 $\pm$ 3) ms) was determined more accurately. By using the newly determined level scheme and halflife, β feedings and reduced Gamow-Teller (GT) transition probabilities (B(GT)) were deduced with higher accuracy. The experimental B(GT) values were confronted with predictions obtained from five shell-model calculations. Two of these theoretical predictions, one using the FPD6* [3] and the other the KB3G [4] interaction, are presented together with the experimental results in Fig. 1. The shell-model calculations include a 'quenching factor' of 0.74 [5]. It was found that the experimental GT-strength distribution over ^{56}Ni states between 3.9 and 6.6 MeV qualitatively agrees
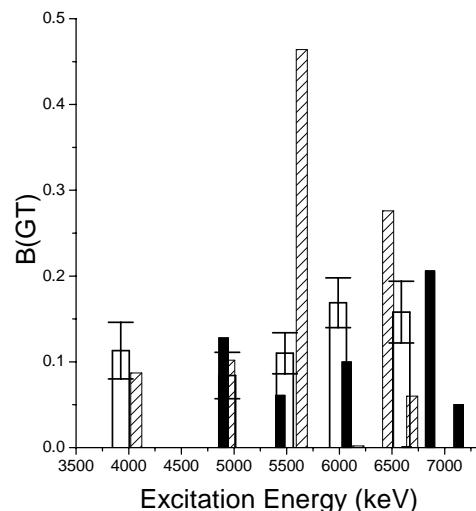

Figure 1: Experimental B(GT)values (empty bars) for the ^{56}Ni levels together with shell-model predictions obtained by using the FPD6* (dashed bars) and KB3G interactions (black bars).

with the predictions (see [2]). We consider this to be a valuable test of shell-model calculations, including their ability to reliably predict the higher-lying GT strength. Moreover, the identification of hitherto unobserved low-spin states in ^{56}Ni is important for further improvement of data from in-beam spectroscopy as well as for further tests of nuclear models. Finally, it was shown [2] that the new experimental data do not imply a revision of the calculated stellar weak-interaction rates of A=56 nuclei [6].

[1] M. Ramdhane *et al.*, Phys. Lett. B 432 (1998) 22
[2] R. Borcea *et al.*, submitted to Nucl. Phys. A
[3] T. Otsuka *et al.*, Phys. Rev. Lett. 81 (1998) 1588
[4] A. Poves *et al.*, nucl-th/0012077, submitted to Nucl. Phys. A
[5] G. Martínez-Pinedo *et al.*, Phys. Rev C 53 (1996) 2602
[6] K. Langanke and G. Martínez-Pinedo, Nucl. Phys. A 673 (2000) 481

Beta-decay properties of ^{60}Ga

C. Mazzocchi[1,2], Z. Janas[1,3], M. Axiotis[4], L. Batist[5], R. Borcea[1], D. Cano-Ott[6], G. de Angelis[4], J. Döring[1], E. Farnea[4,7], A. Faßbender[1], A. Gadea[4,7], H. Grawe[1], A. Jungclaus[8], M. Kapica[1], R. Kirchner[1], J. Kurcewicz[1], S. M. Lenzi[9], T. Martínez[4,7], I. Mukha[1], E. Nácher[7], D. R. Napoli[4], E. Roeckl[1], B. Rubio[7], R. Schwengner[10], J.L. Tain[7], and C.A. Ur[9]

[1]GSI D-64291 Darmstadt, [2]University of Milan, I-20133 Milan, [3]University of Warsaw, PL-00681 Warsaw, [4]LNL- INFN, I-35020 Legnaro, [5]St. Petersburg Nuclear Physics Institute, RU-188-350 Gatchina, [6]Dept. of Nuclear Fission, CIEMAT, E-28040 Madrid, [7]CSIC-University of Valencia, E-46100 Burjassot-Valencia, [8]University of Göttingen, D-37073 Göttingen, [9]University of Padova and INFN, I-35131 Padova, [10]FZ Rossendorf, D-01314 Dresden

The recent progress in experimental and theoretical investigations of N~Z nuclei has been motivated by a rather unique multidisciplinary interest spanning from nuclear-structure physics to fundamental physics, with e.g. tests of the standard model of weak interaction by precision measurements of superallowed $0^+ \rightarrow 0^+$ β decays, and to astrophysics, concerning the EC cooling of supernovae or the astrophysical rp-process. A particularly interesting sample of N~Z nuclei is the series of N=Z - 2 (T_Z= -1) odd-odd nuclei in the fp shell. The isotope ^{60}Ga, which is part of this series, was identified in fragmentation reactions [1,2]. These experiments provided evidence that the ground state is probably bound, but did not yield any decay information. In this contribution we report on preliminary results obtained in the first spectroscopic investigation of the β-decay properties of ^{60}Ga performed at the GSI On-line Mass Separator.

The nucleus ^{60}Ga was produced in the ^{28}Si(^{36}Ar,p3n) fusion-evaporation reaction, induced by a 4.71 MeV/u, 85 particle-nA ^{36}Ar beam. The reaction products were stopped and ionized inside the ion source in two separate experiments:

1. A FEBIAD-E [3] ion source was used. The A=60 beam contained, however, strong isobaric long-lived contaminants of ^{60}Cu and ^{60}Zn.

2. A TIS [3,4] ion source was employed to strongly suppress the A=60 contaminants compared to the values obtained during experiment 1. A suppression factor of 700 for the strongest contaminant ^{60}Cu was reached, while the release efficiency for ^{60}Ga was only reduced by a factor of 6 due to the lower efficiency of thermoionization.

The mass-separated A=60 beam was implanted during consecutive time intervals in two carbon foils each viewed by a ΔE-E silicon telescope for detection of β-delayed protons (βp) in experiment 1 and 2. A total of 613 βp events were collected. By comparing the number of events occurring during the beam-on and beam-off periods in one of the two telescopes (288 events), we determined the half-life of ^{60}Ga to be (70±15) ms.

The investigation of β-delayed γ–rays was also performed in both experiments. Another beam line was used and the detector array consisted of a plastic scintillator surrounded by 13 germanium detectors. Figure 1 shows part of the γ-ray data accumulated as the sum of β-coincident single-hit events. Three γ-lines can clearly be observed, i.e. the known 1004 keV line corresponding to the $2^+ \rightarrow 0^+$ transition in the daughter nucleus ^{60}Zn, the 826 keV line of ^{60}Cu, and the 834 keV line of ^{72}As. The latter one is due to a long-lived contamination from a previous A=72 measurement. Moreover, a 3848(2) keV γ-ray

has been identified, which shows an unambiguous coincidence relationship with the 1004 keV line (see Figure 1). On the basis of these experimental data, we assign the 3848 - 1004keV cascade to the deexcitation of the isobaric analogue state (IAS) in ^{60}Zn. This consideration positions the IAS at 4852(2) keV. By combining this result with Coulomb-energy systematics [5], we deduced a semi-empirical Q_{EC} value of 14176(3) keV for ^{60}Ga. This finding, together with the known [6] mass excess values of ^{60}Zn and ^{59}Zn, yields a mass-excess of –40007(11) keV and a proton separation energy of 36(41) keV for the proton-dripline nucleus ^{60}Ga.
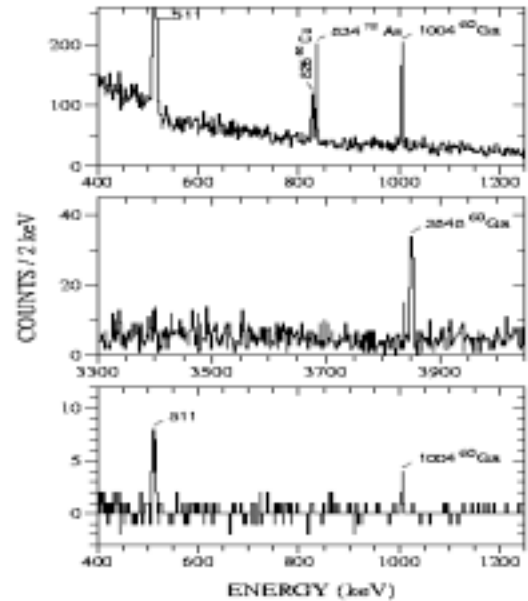

Figure 1. Energy spectrum of β-delayed γ-rays recorded at mass 60. The upper and central panels show parts of the β-coincident γ spectrum, while the lower one displays a background corrected part of the γ spectrum acquired in coincidence with positrons and the 3848 keV γ-ray.

References
[1] B. Blank *et al*, Phys. Rev. Lett. **74**, 4611 (1995)

[2] R. Pfaff *et al*., Phys. Rev. C **53**,1753 (1996)

[3] R. Kirchner *et al*., Nucl. Instr. and Meth. **186**, 295 (1981)

[4] R. Kirchner, Nucl. Instr. and Meth. in Phys. Res. **A** 292, 203 (1990)

[5] M. S. Antony *et al*., At. Data Nucl. Data Tab. **66**, 1 (1997)

[6] G. Audi *et al*., Nucl. Phys. A **624**, 1 (1997)

Beta-decay study of the self-conjugate odd-odd nuclei ^{62}Ga and ^{70}Br

J. Döring[1], C. Plettner[2], M. Axiotis[3], R. Borcea[1], J. Eberth[4], A. Gadea[3], M. Górska[1], H. Grawe[1], Z. Janas[1,5], R. Kirchner[1], M. La Commara[1,6], C. Mazzocchi[1,6], E. Nácher González[1], A. Płochocki[5], E. Roeckl[1], K. Schmidt[1], R. Schwengner[2], T. Steinhardt[4], J. Żylicz[5]

[1]GSI Darmstadt, [2]Forschungszentrum Rossendorf, [3]INFN-LNL Legnaro, [4]Univ. Köln, [5]Warsaw University, [6]Universitá degli Studi di Milano

Nuclei in the mass 70 region exhibit a variety of nuclear structure effects such as rapid shape changes and shape coexistence. Whereas the nuclei around the doubly-magic nucleus ^{56}Ni are considered to be spherical in shape, oblate-deformed ground states have been found in a region around ^{69}Se ($Z = 34$) [1], and prolate-deformed ground states in the proton-rich Sr ($Z = 38$) isotopes [2]. The deformed shapes are well-stabilized by the competing $Z = 34$, 36, and 38 gaps in the single-particle energies. To explore the evolution of the nuclear shape along the $N = Z$ line and their influence on the competition of $T = 0$ and $T = 1$ isospins in odd-odd nuclei, the β-delayed γ-ray emission of the self-conjugate nuclei ^{62}Ga and ^{70}Br has been investigated. The measurements were performed at the on-line mass separator of GSI Darmstadt. Experimental details were reported earlier [3], and preliminary results of the data analysis have been communicated at several conferences [4, 5].

In the experiment on the β^+ decay of ^{62}Ga, an intense 511 keV annihilation peak originating from the $0^+ \to 0^+$ Fermi ground-state decay [6] and the much weaker 954 keV $2^+ \to 0^+$ yrast transition in ^{62}Zn have been identified. If a coincidence gate is set on this 954 keV line, weak γ transitions at 1388 and 2225 keV show up. Thus, the transitions may depopulate levels at 2342 and 3179 keV in ^{62}Zn. From a previous (p,t) reaction study [7], levels at 2330 (0^+) and 3160 keV (2^+) are known in ^{62}Zn which are close in energy to the levels populated in β decay. However, due to limited statistics, no reliable half-life for the β-delayed 954 keV γ ray could be deduced.

The occurrence of the 954, 1388, and 2225 keV transitions can result from two different scenarios: (i) from the β decay of a low-lying isomeric state in ^{62}Ga or (ii) from a non-analog decay branch of the 0^+ ground state in ^{62}Ga to higher-lying 0^+ and/or 1^+ states in ^{62}Zn which are de-excited by the emission of γ rays. If we assume that the observed 954 keV line intensity results from a non-analog decay branch, then a branching ratio of $(0.106 \pm 0.017)\%$ can be estimated. This ratio agrees quite well with a previously reported value of $(0.120 \pm 0.021)\%$ [8]. Since almost the same ratio has been obtained in two very different measurements, the interpretation as a non-analog branch is favoured.

In the study of the lightest proton-bound bromine isotope, ^{70}Br, extensive β-γ-γ coincidences have been measured for the decay of the known $T_{1/2} = 2.2(2)$ s isomer [9]. The analysis reveals a complex decay scheme with about 74% of the β feeding populating the 4606 keV level in ^{70}Se which is known as a $(8,9^+)$ state from previous in-beam work [10]. This level was found to be depopulated by transitions of 569.0 and 690.2 keV. However, we observe additional γ rays of 958 and 1604 keV which link

this level further to the yrast 6^+ and the 6_2^+ states in ^{70}Se, and thus restrict spin and parity to $I^\pi = 8^+$. Furthermore, the yrast sequence in ^{70}Se has been observed up to the 10^+ state at 5207 keV for the first time in β decay. The deduced β feeding of the 10^+ level is about 1.2(2)%. The spectrum of γ rays in coincidence with the 1169 keV $10^+ \to 8^+$ transition is displayed in Fig. 1 which clearly shows all lower-lying transitions of the yrast sequence in ^{70}Se. Thus, the β-decaying isomeric state in ^{70}Br must
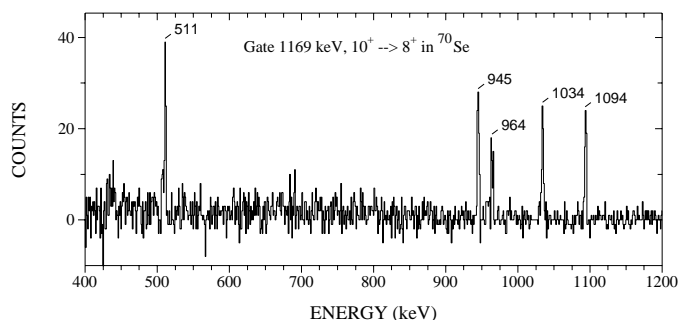

Figure 1: Background-corrected γ-ray spectrum in coincidence with β rays and the $10^+ \to 8^+$ γ transition in ^{70}Se.

have a high spin, and we propose spin and parity of 9^+, the only assignment being consistent with all experimental results. The high spin of the isomer is interpreted as arising from the Nilsson configuration ($\pi 9/2^+[404]$, $\nu 9/2^+[404]$) at an oblate deformation of $\beta_2 \approx -0.3$. Our findings are in agreement with very recently reported conclusions from another experiment [11] where also a 9^+ assignment is proposed. However, this is at variance with the earlier assignment of 5^+ given by the same group [12].

References

[1] M. Wiosna et al., Phys. Lett. B **200** (1988) 255.

[2] C.J. Lister et al., Phys. Rev. Lett. **49** (1982) 308.

[3] J. Döring et al., GSI Scientific Report 2000, p. 14.

[4] E. Roeckl et al., Nucl. Phys. A (in press).

[5] J. Döring et al., Proc. Pingst2000, Report of Lund Uni., p. 131.

[6] C.N. Davids et al., Phys. Rev. C **19** (1979) 1463.

[7] R.A. Hinrichs et al., Phys. Rev. C **10** (1974) 1381.

[8] B.C. Hyman et al., Cyclotrone Inst., Texas A&M Univ., Progress in Research 1999, p. I-28.

[9] B. Vosicki et al., Nucl. Instrum. Meth. **186** (1981) 307.

[10] T. Mylaeus et al., J. Phys. G **15** (1989) L135.

[11] A. Piechaczek et al., Phys. Rev. C **62** (2000) 054317.

[12] A. Piechaczek et al., Proc. Conf. on Perspectives in Nucl. Phys., World Scientific, Singapore, 1999, p. 201.

Beta decay of ^{96}Ag isomers and delayed proton emission to ^{95}Rh levels

L. Batist [1], C.R. Bingham [2], R. Borcea [3], J. Döring [3], M. Gierlik [4], H. Grawe [3], K. Hauschild [5], Z. Janas [3,4]
M. Karny [2,4], R. Kirchner [3], M. La Commara [3,6], C. Mazzocchi [3], F. Moroz [1], E. Roeckl [3], K. Schmidt [3,7]
[1] PNPI Gatchina, [2] University of Tennessee, [3] GSI Darmstadt, [4] University of Warsaw, [5] DAPNIA/SPhN
CEA Saclay, [6] University Frederico II Naples, [7] University of Edinburgh

The decay of ^{96}Ag was first investigated by Kurcewicz et al. [1], who measured a half-life of 5.1(4) s and observed the emission of β-delayed γ rays (βγ) and β-delayed protons (βp). Later on, Schmidt et al. [2] inferred a half-life of 5.22(15) s from βp data, and found it to be different from the weighted mean (4.50(6) s) of the half-lives of the βγ transitions, indicating the existence of two decaying states in ^{96}Ag. This result is in agreement with shell-model calculations, which predict two closely spaced 2$^+$ and 8$^+$ states to occur at low ^{96}Ag excitation-energy. However, the previous works [1,2] did not draw definite conclusions concerning the two ^{96}Ag states. The aim of the present study was to clarify the decay characteristics of these isomers by reinvestigating their βγ and βp properties. We used a total absorption γ-ray spectrometer (TAS) [3]. TAS was expected to be more suitable for this purpose as it is capable of detecting the whole γ cascade following the β decay rather than individual γ transitions. Concerning the βp decay, a coincidence condition between a proton detector and TAS was used. This condition was expected to select the cascades of γ rays de-exciting the ^{95}Rh levels populated by proton emission.

The neutron-deficient isotope ^{96}Ag was produced by fusion-evaporation reactions of a ^{40}Ca beam from the heavy-ion accelerator UNILAC with a ^{60}Ni target. The reaction products were separated at the GSI on-line mass separator by using a chemically selective FEBIAD ion source. The mass-separated A=96 beam was implanted into a transport tape, with the resulting radioactive sources being periodically moved from the collection position to the centre of the TAS, where it was viewed by two 0.5 mm thick silicon detectors. One of them, placed at the side of the tape where the ions had been implanted, was used to detect positrons and protons. The other detector placed at the opposite side of the tape served to record positrons and thus distinguish the protons emitted after β$^+$ decay from those related to EC decay.

The ^{96}Pd levels populated via ^{96}Ag β-decay are shown in Fig. 1. The analysis of TAS spectra yields evidence for β feeding of both the 2$^+$ and 8$^+$ levels in ^{96}Pd. This result indicates β-decaying isomers in ^{96}Ag with low and high spin, respectively. The ^{95}Rh levels populated via βp emission are also displayed in Fig. 1. The strongly populated ^{95}Rh level at 1350 keV can be unambiguously related to the 13/2$^+$ level established by in-beam spectroscopy [4]. Besides the agreement in energy, this assignment is supported by the observation that the decay curve for this level is similar to that for the 8$^+$ ^{96}Pd level. Several new ^{95}Rh levels have been found in addition to those established earlier by in–beam spectroscopy and β decay of ^{95}Pd. One of them, the strongly populated 680 keV level shows the same decay characteristics as that observed for the β feeding to the 2$^+$ ^{96}Pd level. The evident shell-model counterpart to this level is that with a spin-parity assignment of 7/2$^+$ and calculated energy of 650 keV [5], which corresponds to the first excited state

built on the proton $g_{9/2}$ single-particle ground state. Tentative spin assignments of 5/2$^+$ and 11/2$^+$ can be deduced for the other new ^{95}Rh levels on the basis of the comparison with shell-model predictions [5], and by taking into account that they are not populated by the yrast cascade identified by in-beam spectroscopy.

The half-life of the high-spin isomer was determined by evaluating the time characteristics of the β$^+$ feeding to the ^{96}Pd 8$^+$ level. The half-life of the low-spin isomer was deduced by using the decay curves of the TAS peak corresponding to the 2$^+$ ^{96}Pd level and the 680 keV (7/2$^+$) ^{95}Rh state. The βp branching ratios, indicated in Fig.1 for both isomers of ^{96}Ag, were determined on the basis of a decomposition of the decay curves for βp events and positron-coincident γ rays detected by TAS. The additional uncertainties, which are due to the non-observation of EC-delayed γ rays, were estimated not to exceed 10% of the presented values. Making use of the new half-lives and branching ratios, one can estimate that the summed βp Gamow-Teller strengths for the two isomers are remarkably different. This result probably points to the effect of proton-γ competition for highly excited ^{96}Pd levels.
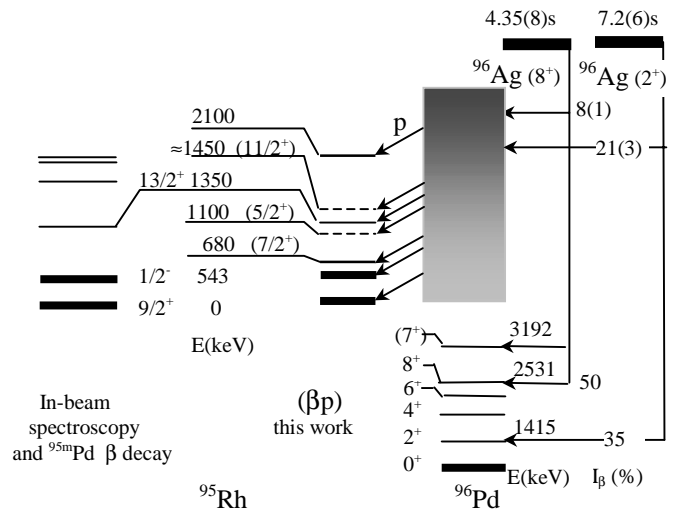

Fig. 1. Excited states in ^{96}Pd and ^{95}Rh populated by the ^{96}Ag β decay and β-delayed proton emission. For unbound ^{96}Pd levels, only βp-intensities are presented.

[1] W. Kurcewicz et al., Z. Phys. A 308 (1982) 21.
[2] K. Schmidt et al., Nucl. Phys. A 624 (1997) 185.
[3] M. Karny et al., Nucl. Instr. and Meth. Phys. Res., B 126 (1997) 320.
[4] H.A. Roth, Phys. Rev., C50 (1994) 1330.
[5] I.P. Johnstone and L.D. Skouras. Phys. Rev, C55 (1997) 1227.

The β^+/EC decay of ^{100}In and the ^{100}Sn shell model

J. Döring[1], C. Plettner[1,2], V. Belleguic[3], H. Grawe[1], L. Batist[4], R. Borcea[1],
M. Górska[5], N. Harrington[6], Z. Janas[1,7], R. Kirchner[1], C. Mazzocchi[1,8], P. Monroe[6], E. Roeckl[1],
Ch. Schlegel[1], K. Schmidt[1,6], R. Schwengner[2]

[1]GSI, D-64291 Darmstadt, [2]FZ Rossendorf, D-01314 Dresden, [3]Université de Paris-Sud, F-91405 Orsay,
[4]PNPI, RU-188-350 Gatchina, [5]IKS KU Leuven, B-3001 Leuven, [6]University of Edinburgh, Edinburgh EH9 3JZ, UK,
[7]University of Warsaw, PL-00681 Warsaw, [8]University of Milan, I-20133 Milan

The nucleus ^{100}In, the neutron-proton particle-hole (*ph*) neighbour of the doubly magic ^{100}Sn, is the closest lying neighbour which can be studied today in β^+/EC decay with rates allowing detailed $\beta\gamma\gamma$ spectroscopy, while still having a simple *ph* shell-model structure. Its ground state is expected to be the $I_{max} - 1 = 6^+$ respectively 7^+ member of the $[\pi g_{9/2}^{-1} \nu d_{5/2}]_{2-7}$ or $[\pi g_{9/2}^{-1} \nu g_{7/2}]_{1-8}$ multiplets (Fig. 1). Their centroids are predicted to be nearly degenerate [1, 2]. The Gamow-Teller (GT) decay of a $\pi g_{9/2}$ proton in ^{100}In to a $\nu g_{7/2}$ neutron in ^{100}Cd will preferably populate either the $I^\pi = (5 - 7)^+$ members of the two-quasiparticle configurations $\nu d_{5/2} g_{7/2}$ or $\nu g_{7/2}^2$ or the four-quasiparticle GT resonance, where these configurations are coupled to an unpaired $\pi g_{9/2}^{-2}$ proton state. The two-quasiparticle $I^\pi = (5 - 7)^+$ states in the daughter nucleus ^{100}Cd have simple configurations, which are easily accessible to shell-model interpretation [3, 4]. They are lying well below the GT resonance in a region of low level density, so that their GT feeding and γ decay can be used to assign configurations to parent and daughter states.
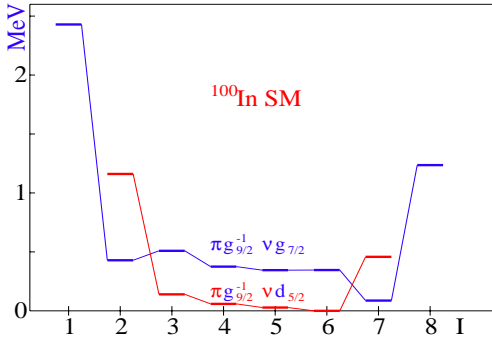

Figure 1: States from the $\pi g_{9/2}^{-1}\ \nu g_{7/2}$ and $\pi g_{9/2}^{-1}\ \nu d_{5/2}$ multiplets as predicted by the shell model

We have performed a study of the ^{100}In β^+/EC decay at the GSI on-line mass separator. The reaction ^{50}Cr(^{58}Ni,αp3n) at 6.15·A MeV energy and 45 particle-nA intensity of the ^{58}Ni beam was used to produce mass separated ^{100}In at an average rate of 5 atoms/s from a TIS ion source [5]. The ^{100}In samples were collected and measured in grow-in mode in cycles of 16 s on a movable tape and then removed to suppress long-lived daughter activity. The collection point was surrounded by a plastic scintillator to detect positrons with 70 % efficiency. Two composite HPGe detectors, a cluster of the EUROBALL type and a superclover from the VEGA array, a large volume single HPGe and a LEPS detector served for γ-ray detection with a total detection efficiency of 3.7 % for a 1.33 MeV γ ray.

A γ-coincidence spectrum gated by positrons and the $2^+ \rightarrow 0^+$ γ transition in the daughter ^{100}Cd is shown in Fig. 2. This nucleus has been well studied in in-beam spectroscopy up to high spin [3, 4]. A strong apparent GT feeding of the known $I^\pi = 6^+$ and 8^+ states is clearly observed. From the preliminary analysis of the feeding pattern a spin and parity assignment of $I^\pi = (7^+)$ is inferred for the parent state in ^{100}In. A halflife analysis of the strong 297, 795 and 1005 keV γ lines yields a value of 5.1(5) s in agreement with the adopted average of previous results 6.1(7) s [6].
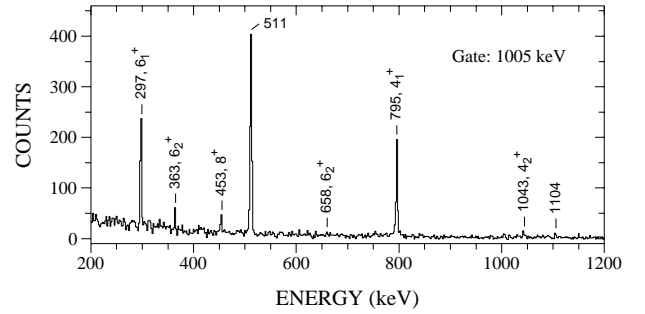

Figure 2: Partial β-gated $\gamma\gamma$ spectrum of the ^{100}In decay gated on the $2^+ \rightarrow 0^+$ transition in the daughter ^{100}Cd

The spin and parity assigned to the parent state, which could be the ground state or an isomer, is clearly at variance with the shell-model prediction shown in Fig. 1 [1]. The residual interactions used in shell-model calculations favour $I^\pi = 6^+$ [1, 7, 8] in agreement with tentative assignments to the odd-odd In isotopes and N=51 isotones. The *ph* nature of the interaction requires that the two assignments belong to different configurations (Fig. 1). This excludes a trivial solution to the problem by shifting the centroids of the multiplets, as the configuration mixing would counteract, and would rather indicate a revision of the realistic interaction used in the shell model.

References

[1] M. Górska et al., Proc. ENPE 99, eds. B. Rubio, M. Lozano, W. Gelletly, AIP Conf. Proc. **495** (1999) 217

[2] H. Grawe et al., Proc. SM2K, RIKEN, ed. T. Otsuka, Nucl. Phys. A, in print

[3] M. Górska et al., Z. Phys. **A350** (1994) 181

[4] R.M. Clark et al., Phys. Rev. **C61** (2000) 044311

[5] R. Kirchner, Nucl. Instr. and Meth. **A292** (1990) 203

[6] G. Audi et al., Nucl. Phys **A624** (1997) 1

[7] H. Grawe et al., Physica Scripta **T56** (1995) 71

[8] B.A. Brown and K. Rykaczewski, Phys. Rev. **C50** (1994) R2270

Halflives of neutron deficient nuclei near ^{100}Sn

E. Wefers[1], T. Faestermann[1], R. Schneider[1], A. Stolz[1], K. Sümmerer[2], J. Friese[1], H. Geissel[2],
M. Hellström[3], P. Kienle[1], H.-J. Körner[1], M. Münch[1], G. Münzenberg[2], P. Thirolf[4] and H. Weick[2]

[1]TU München, [2]GSI, [3] University of Lund, [4] LMU München

Neutron deficient nuclei near ^{100}Sn have been produced by fragmentation of a 1 A·GeV ^{112}Sn beam in a beryllium target, separated in the FRS and identified with a new detector system [1]. The unambiguously identified ions were stopped in a highly segmented silicon detector stack [2]. We determined the halflives for each implanted isotope using a maximum likelihood method [3].

Fig. 1 shows the measured isotopic yields for fragments from strontium to indium. The cross sections extracted from these yields are in good agreement with empirical predictions (EPAX). The spectra show the previously unobserved $N = Z - 2$ nuclei ^{76}Y (2 events) and ^{78}Zr (one event). Due to the excellent resolution of our identification detectors we can assign a 3σ confidence level to these observations. In addition fig. 1 demonstrates the absence of the $N = Z - 1$ nuclei ^{81}Nb, ^{85}Tc and ^{89}Rh, which are probably unstable against proton emission.
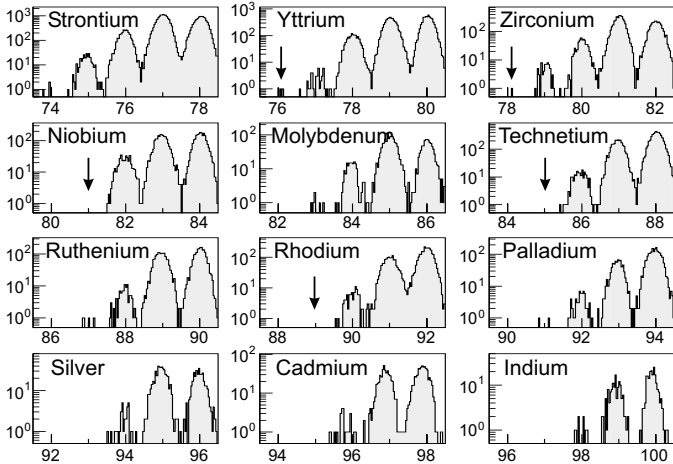

Figure 1: Mass spectra of the observed ions between Sr and In. The arrows indicate the identification of ^{76}Y and ^{78}Zr and the absence of ^{81}Nb, ^{85}Tc and ^{89}Rh.

The identification of ^{76}Y and ^{77}Y coincides with recent predictions of the relativistic Hartree-Bogoliubov model for the proton dripline [4], whereas ^{81}Nb and ^{85}Tc are not predicted to be dominantly proton emitters.

For the identified nuclides as well as for the unobserved ones we determined limits for their halflives resulting from their flight time through the FRS (table 1). Note that the failure to observe ^{89}Rh could also be due to the small cross section expected (50 pb) just at our detection limit. In order to improve our knowledge on the proton dripline we implanted the $N = Z - 1$ nuclei ^{75}Sr, ^{77}Y, ^{79}Zr and ^{83}Mo into the Si detector stack. The measured halflives, which are as short as expected for β-decays between mirror nuclei, are also listed in table 1. For ^{77}Y we collected 12 nuclei which decay all via β-decay, setting an upper limit

	$T_{1/2}$		$T_{1/2}$		$T_{1/2}$
^{75}Sr	80^{+400}_{-40} ms	^{76}Y	> 170 ns	^{77}Y	57^{+22}_{-12} ms
^{78}Zr	> 170 ns	^{79}Zr	80^{+400}_{-40} ms	^{81}Nb	< 44 ns
^{83}Mo	6^{+30}_{-3} ms	^{85}Tc	< 110 ns		

Table 1: Halflives of $N < Z$ nuclei. For details see text.

to a possible proton branch of 10% (1σ c.l.).

An important nuclear physics input quantity for network calculations modelling the astrophysical rp-process are the halflives of the so-called waiting point nuclei. We measured the halflives of all these nuclei from ^{80}Zr up to ^{92,93}Pd. In addition we were able to determine halflives of several unknown indium, rhodium and technetium isotopes near the $N = Z$-line with the same magnet settings of the FRS. These results are listed in table 2.

	$T_{1/2}$ [s]		$T_{1/2}$ [s]		$T_{1/2}$ [s]
^{80}Zr	$5.3^{+1.1}_{-0.9}$	^{84}Mo	$3.7^{+1.0}_{-0.8}$	^{87}Tc	2.18 ± 0.16
^{88}Ru	$1.2^{+0.3}_{-0.2}$	^{89}Ru	1.45 ± 0.13	^{91}Rh	1.74 ± 0.14
^{92}Rh	5.6 ± 0.5	^{93}Rh	13.9 ± 1.6	^{92}Pd	$1.0^{+0.3}_{-0.2}$
^{93}Pd	1.0 ± 0.2	^{99}In	$3.0^{+0.8}_{-0.7}$		

Table 2: Halflives of nuclei near the $N = Z$ line.

In an earlier report of preliminary results [5], an erroneous value for the ^{93}Pd and ^{92,93}Rh halflife was given because some daughter decays were included and the background suppression was insufficient in the first analysis.

To investigate superallowed Fermi-β-decays we studied the six heaviest candidates of $N = Z$ odd-odd nuclei between ^{78}Y and ^{98}In. For the first time we observed fast transitions, compatible with superallowed Fermi transitions for ^{90}Rh, ^{94}Ag and ^{98}In. In addition to these fast transitions, we have observed a few long-lived isomeric states. The measured halflives are listed in table 3.

	$T_{1/2}$[ms]	$T_{1/2}^{\text{iso}}$[s]		$T_{1/2}$[ms]	$T_{1/2}^{\text{iso}}$[s]
^{78}Y	55^{+9}_{-6}	$5.7^{+0.7}_{-0.6}$	^{82}Nb	48^{+8}_{-6}	
^{86}Tc	59^{+8}_{-7}		^{90}Rh	12^{+9}_{-4}	$1.0^{+0.3}_{-0.2}$
^{94}Ag	26^{+26}_{-9}	$0.45^{+0.20}_{-0.13}$	^{98}In	32^{+32}_{-11}	$1.2^{+1.2}_{-0.4}$

Table 3: Halflives of $N = Z$ odd-odd nuclei.

References

[1] A. Stolz et al., GSI Scientific Report 1998, p.174

[2] E. Wefers et al., GSI Scientific Report 1998, p.173

[3] A. Stolz, PhD thesis, TU München (2001)

[4] G.A. Lalazissis et al., Nucl. Phys. A679 (2001) 481

[5] E. Wefers et al., AIP Conference Proc. 495 (1999) 375

Alpha decay of ^{114}Ba

C. Mazzocchi[1,2], Z. Janas[1,3], L. Batist[4], V. Belleguic[2], J. Döring[2], M. Gierlik[1], M. Kapica[1], R. Kirchner[1], H. Mahmud[5], E. Roeckl[1], K. Schmidt[5], P.J. Woods[5], and J. Żylicz[1]

[1]GSI D-64291 Darmstadt, Germany, [2]University of Milan, I-20133 Milan, Italy, [3]University of Warsaw, PL-00681 Warsaw, Poland, [4]St. Petersburg Nuclear Physics Institute, RU-188-350 Gatchina, Russia, [5]University of Edinburgh, Edinburgh EH9 3JZ, UK

In recent years, intense experimental and theoretical research has been devoted to investigate nuclei near the doubly magic nucleus ^{100}Sn (Z=N=50). In this region of the nuclear chart, an island of α emission occurs, covering neutron-deficient isotopes of tellurium (Z=52) through cesium (Z=55). Alpha emission is a rich source of nuclear structure information [1]. The α-particle energy E_α, corrected for the recoil effect, yields the difference between the masses of mother and daughter nucleus. Above ^{100}Sn, this quantity directly relates to the Z=N=50 shell-strength. Moreover, the information on energy, half-life and α-decay branching ratio (b_α) yields the reduced widths for this disintegration mode (W_α). Measurements of W_α values may shed light on the question whether superallowed α decay occurs for nuclei beyond ^{100}Sn, with protons and neutrons occupying identical $d_{5/2}$, $d_{3/2}$ and $g_{7/2}$ orbitals. Moreover, these nuclei, and in particular ^{114}Ba, are predicted to be promising candidates for the observation of cluster (^{12}C) radioactivity. The decay of ^{114}Ba had already been investigated in previous experiments [2-4], but only lower limits for α and ^{12}C partial half-lives could be established [2]. In this contribution we report on preliminary results obtained in a reinvestigation of the α-decay properties of ^{114}Ba.

The experiment was performed at the GSI On-line Mass Separator. ^{114}Ba was produced in fusion-evaporation reactions induced by a 284 MeV ^{58}Ni beam on 2.0-3.8 mg/cm^2 thick ^{58}Ni targets. The reaction products were stopped inside a high-temperature cavity ion source in two tantalum catcher foils, from which most recoils – at the ion source temperature of about 2400 K – are swiftly released as thermalized atoms. Chemical selectivity for barium isotopes was achieved by adding CF$_4$ and thus using on-line fluorination. The ionization takes place selectively in the fluorination sideband of BaF, all contaminants including CsF being reduced to levels well below 10^{-5} [5]. The BaF$^+$ ions were accelerated to 55 keV, mass-separated and focused alternately onto two carbon foils, each one being viewed by a ΔE-E silicon telescope.

The search for α emission was performed using the ΔE spectrum registered in anticoincidence with the E detector. Figure 1 shows the corresponding spectrum obtained from both telescopes during a measurement time of 55.6 hours. Three α lines were observed at the energies 3410±40, 3740±30 and 4160±30 keV, containing 38, 21 and 22 events, respectively. We assign the lowest-energy line to the α decay of ^{114}Ba. This assignment is based on the Z and A selectivity that was reached combining the fluorination ion source with mass-separation. The higher-energy members of this triplet are assigned to the known [6] α lines from the decay of ^{110}Xe and ^{106}Te. Taking into account the recoil correction, we obtained a Q_α value of 3540±40 keV for ^{114}Ba. This result, together with the known [6] Q_α values of ^{110}Xe and ^{106}Te, yields a Q value of 19000±60 keV

for ^{12}C decay of ^{114}Ba, which is important to obtain experimentally relevant predictions for this decay mode.
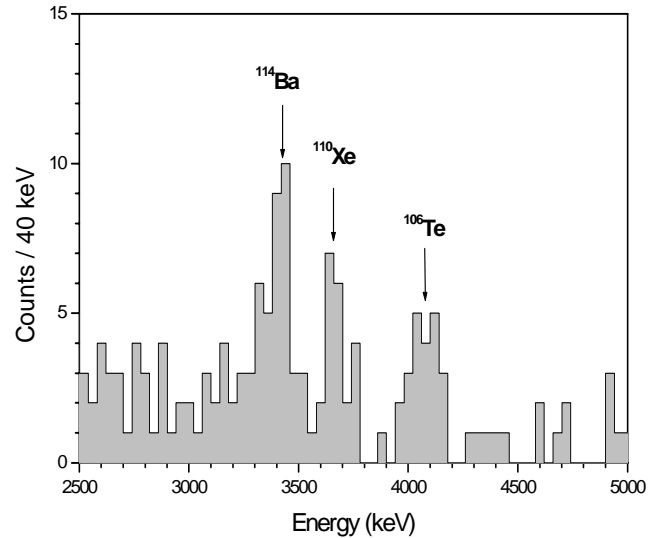

Figure 1. Section of the ΔE spectrum from both telescopes, taken in anticoincidence with the related E detectors.

By comparing the 38 α events observed with the 980 β-delayed protons (βp) detected simultaneously in ΔE-E coincidence, the b_α value of ^{114}Ba was determined to be $(9\pm3)\cdot10^{-3}$. This result takes into account the detection efficiencies of the telescopes and the known βp branching ratios for ^{114}Ba [4] and its daughter ^{114}Cs [7]. The new b_α value is somewhat larger but still compatible with the previously obtained upper limit of $3.7\cdot10^{-3}$ (68% c.l.) [2]. Moreover, the analysis of time correlations will allow us to deduce the half-life of ^{110}Xe and the b_α values for ^{110}Xe and ^{106}Te.

References

[1] E. Roeckl, Alpha decay, in: *Nuclear Decay Modes*, ed. D.N. Poenaru, IOP, 1996, pp. 237

[2] A. Guglielmetti et al., Phys. Rev. C **52** (1995) 740

[3] A. Guglielmetti et al., Phys. Rev. C **56** (1997) R2912

[4] Z. Janas et al., Nucl. Phys. A **627** (1997) 119

[5] R. Kirchner, Nucl. Instr. Meth. B **126**, 135 (1997)

[6] D. Schardt et al., Nucl. Phys. A **368**, 153 (1981)

[7] E. Roeckl et al., Z. Phys. A **294** (1980), 221

A new micro-second isomer in neutron-rich ^{136}Sb

M.N. Mineva[1], M. Hellström[1,2], M. Bernas[3], J. Gerl[2], H. Grawe[2], M. Pfützner[4], P.H. Regan[5],
D. Rudolph[1], J. Genevey[6], Z. Janas[4], J. Kurcewicz[4], P. Mayet[2], J.A. Pinston[6], Zs. Podolyàk[5],
M. Rejmund[7], Ch. Schlegel[2], K. Sümmerer[2]

[1]Lund University, [2]GSI-Darmstadt, [3]IPN Orsay, [4]Warsaw University,
[5]University of Surrey, [6]ISN Grenoble, [7]CEA Saclay

By studying the properties and decay patterns of isomeric states resulting from the coupling of valence particles in high-j orbitals at the $Z = 50$ and $N = 126$ shell closures, valuable information on nuclear structure and nucleon-nucleon interaction in very neutron-rich systems can be obtained. In December 1999, we therefore performed an experiment at GSI to search for new, relatively long-lived (100ns - 100μs) isomeric states in the region around the neutron-rich doubly magic nucleus ^{132}Sn. The nuclei of interest were produced by projectile fission of ^{238}U at 750 MeV/u in a 1.0 g/cm^2 ^{9}Be target, separated using the Fragment Separator (FRS) and implanted in a catcher at the final focus surrounded by Ge detectors. More details about the experiment are given in [1, 2].

The well-known decay of the $I^\pi = 19/2^-$ isomer in ^{135}Te [3] was used to verify the particle identification and lifetime determination procedures. Figure 1 shows the γ-spectra recorded in delayed coincidence with ions of ^{135}Te and ^{136}Sb implanted in the catcher. A previously unknown delayed γ-transition at 173 keV is clearly seen in the ^{136}Sb-gated spectrum.
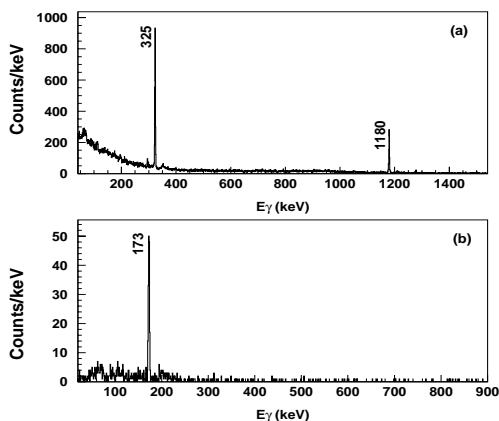

Figure 1: Delayed γ-ray spectra measured in coincidence with implanted ^{135}Te (a), and ^{136}Sb (b) ions. The time-delay is 250 ns, and 500 ns, respectively. The energy labels are in keV.

The decay curves of ^{135}Te and ^{136}Sb are presented in figure 2. The distributions were fitted to obtain the corresponding half-lives of the isomeric decays, and the results are summarized in Table 1. The half-life of the proposed new isomeric state in ^{136}Sb is $T_{1/2}$=566±46 ns [2].

The β-decay of the ^{136}Sb ground state was studied by Hoff et al. [4], who suggest it is the $I^\pi = 1^-$ member of the $\pi g_{7/2}\nu f_{7/2}^3$ multiplet. Previous to our experiment, however, no excited states were known. The energy (173 keV) and half-life (566 ns) of the single delayed γ-ray we observe
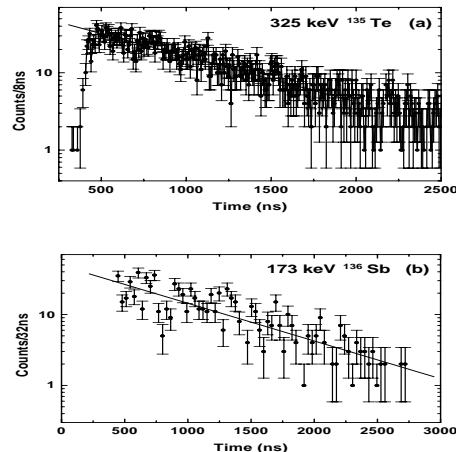

Figure 2: Time distribution curves of a) the 325 keV line from the decay of the $I^\pi = 19/2^-$ isomer in ^{135}Te and b) the 173 keV line identified in ^{136}Sb.

Table 1: Determined isomer half-lives

Isotope	I^π	$T_{1/2}$ (ns) (this work)	$T_{1/2}$ (ns) (previous)
^{135}Te	$19/2^-$	512±22	510±20 [3]
^{136}Sb	-	566±46	-

make it an unlikely candidate for the transition deexciting the isomeric state. More likely, the primary isomeric transition has low energy (<50 keV) and escapes detection in our setup due to internal conversion or absorption.

To help in interpreting the experimental observations we have performed spherical shell model calculations, using two different sets of interactions, to calculate the excitation energies for the $\pi g_{7/2}\nu f_{7/2}^3$ multiplet members. The calculations indicate that the isomer may have $I^\pi = 6^-$, and the observed 173 keV γ-ray could be the $4^- \rightarrow 2^-$ transition. However, although ^{136}Sb has only one proton and three neutrons outside the doubly magic ^{132}Sn core, the gradual onset of collectivity as more valence particles are added could influence the level ordering and spacing. More experimental studies of ^{136}Sb are clearly needed.

References

[1] M.N. Mineva *et al.*, *Proc. 2nd International Balkan School on Nuclear Physics*, Bodrum, Turkey, September 2000, Balkan Physics Letters, in press.

[2] M.N. Mineva *et al.*, to be submitted to EPJ A.

[3] K. Kawade *et al.*, Z. Phys. A **298**, (1980) 273.

[4] P. Hoff *et al.*, Phys. Rev. C **56**, (1997) 2865.

High Spin States Populated via Projectile Fragmentation in Very Neutron-Rich Nuclei Around Mass 180

P. Mayet[1], J. Gerl[1], Ch. Schlegel[1], Zs. Podolyák[2], P.H. Regan[2], M. Caamaño[2], M. Pfützner[3], M. Hellström[1], M. Mineva[4] for the GSI ISOMER collaboration

K-isomers can be found mainly in the A∼180 region. The best examples of K-isomerism are predicted to occur on the neutron-rich side of the valley of stability and are thus barely reachable by standard nuclear reactions like deep inelastic reactions. Up to now, only projectile fragmentation has proven to be an efficient method in populating heavy neutron-rich isotopes with cross-sections sufficient to perform γ-ray spectroscopy. Thus, the FRagment Separator [1] (FRS) associated with γ-ray spectroscopy techniques has been successfully used at GSI to search for K-isomers with lifetimes ranging from nano- to milliseconds in the mass region around A∼180.

These isomers were produced following the fragmentation of a 1 GeV/nucleon ^{208}Pb beam impinging on a 1.6 g/cm^2 Be target. The fragments were separated through the FRS working in achromatic mode and identified using the Bρ-ΔE-TOF method. Ions were stopped in a 5 mm thick Al catcher covering an implantation area of 16 cm on horizontal position. Prompt and delayed γ-rays in coincidence with implanted ions of interest were measured using a Segmented Clover Array whose efficiency was about 6% at 1.33 MeV for the central position of the catcher.

Several new isomers were observed in neutron-rich A=180-200 nuclei, as shown in the following figure, providing the first nuclear structure information from the successive γ-decay cascade. In particular, the rotational band of ^{190}W [2] has been observed for the first time.

Moreover, the ability of this novel method to reach high spin states has been demonstrated by populating K=$\frac{35}{2}^-$ isomeric state in ^{175}Hf [3], ^{179}W [4] and ^{181}Re [5]. This spin represents the highest value observed so far in projectile fragmentation.

Institutes :
[1]*GSI, Planckstrasse 1, D-64291 Darmstadt, Germany, contact person: P.Mayet@gsi.de*
[2]*Dept. of Physics, University of Surrey, Guildford, GU2 5XH, UK*
[3]*Institute of Experimental Physics, Warsaw University, Pl-00861 Warsaw, Poland*
[4]*Div. of Cosmic and Subatomic Physics, Lund University, SE-22100, Sweden*

References:
[1] H. Geissel *et al.*, Nucl. Inst. Meth. B **70**, 286 (1992).
[2] Z. Podolyák *et al.*, Phys. Lett. **B491**, 225 (2000).
[3] G.D. Dracoulis and P.M. Walker, Nucl. Phys. A **342**, 335 (1980).
[4] P.M. Walker *et al.*, Nucl. Phys. A **568**, 397 (1994).
[5] C.J. Pearson *et al.*, Phys. Rev. Lett. **79**, 605 (1997).
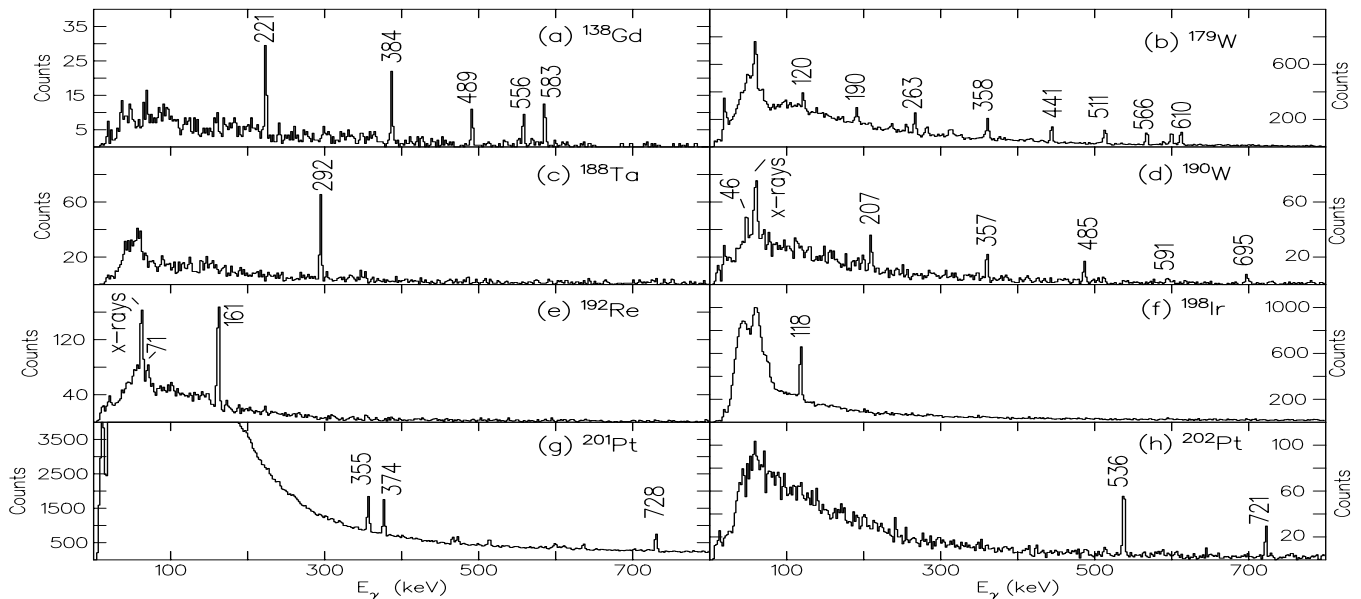
New microsecond isomers in ^{189,190}Bi

A.N. Andreyev[1,5], D. Ackermann[2], P. Cagarda[3], J. Gerl[2], F. P. Heßberger[2], S. Hofmann[2], K. Heyde[4],
M. Huyse[1], A. Keenan[5], H. Kettunen[6], A.Kleinböhl[2], A. Lavrentiev[7], M. Leino[6], B. Lommel[2], M. Matos[3],
G.Münzenberg[2], C. Moore[5], C. D. O'Leary[5], R. D. Page[5], S. Reshitko[2], S. Śaro[3], C. Schlegel[2],
H. Schaffner[2], M. Taylor[5], P.Van Duppen[1], L. Weissman[1], R. Wyss[8]

[1]Instituut voor Kern- en Stralingsfysica, University of Leuven, Belgium; [2]GSI Darmstadt, Germany;
[3]Comenius University of Bratislava, Slovakia; [4]Institute for Theoretical Physics, Gent, Belgium, [5]Oliver
Lodge Laboratory, University of Liverpool, United Kingdom; [6]University of Jyväskylä, Finland; [7]JINR,
Dubna, Russia; [8]Royal Institute of Technology, Stockholm, Sweden

New microsecond isomers in the neutron-deficient isotopes ^{189,190}Bi have been identified at the velocity filter SHIP in the p4n and p3n evaporation channels, respectively, of the complete fusion reaction of ^{52}Cr ions with a ^{142}Nd target. After in-flight separation the evaporation residues (EVRs) were implanted into a position-sensitive silicon detector (PSSD), where their subsequent α-decays were measured. Behind the PSSD a four-fold segmented Ge-clover detector was installed for prompt and delayed (up to 5 ms) α–γ and α–X ray coincidence measurements allowing for the investigation of long-lived isomeric states. EVRs were identified by excitation-function measurements and by using the Recoil-Decay-Tagging method on the basis of delayed recoil-γ, recoil-X ray, and recoil-γ-α coincidences. A detailed description of the experimental set-up used and of the results for ^{188,189,190}Po and their daughter products was given in [1].

Fig.1a shows the γ-ray spectrum measured by the clover detector in coincidence with recoils registered in the PSSD. The γ-transition observed at 357(1) keV has an excitation function similar in shape and position to the 6672-keV α-decay of the $9/2^-$ ground state of ^{189}Bi ($T_{1/2} = 680$ ms) and of the 7298 keV α-decay of the $1/2^+$ isomeric state (^{189m1}Bi) of ^{189}Bi. On this basis we assign this transition to ^{189}Bi. Fig.1b shows the same spectrum as in Fig.1a, but with an additional condition that the EVR-γ pair is correlated within the time interval of 2 s with an α decay of $E_\alpha = 6672$ keV. The procedure to take into account the background of possible random correlations is described in detail in [2]. In Fig.1b, besides a peak at $E_\gamma = 357(1)$ keV coincidences with the K-X rays of Bi are also observed. Thus, the excitation function behaviour, coincidence with the Bi K-X rays and the condition of correlation with the α decay of ^{189g}Bi establishes the origin of the 357 keV γ-line as an isomeric state (^{189m2}Bi) built on top of the $9/2^-$ ground state in ^{189}Bi.

By comparing the number of the K-X rays and γ–rays in Fig.1b, corrected for the corresponding efficiencies [1], a conversion coefficient of $\alpha_K = 0.9(1)$ was deduced, which is consistent with the theoretical value of $\alpha_K(357$ keV, M2$) = 0.77$. This establishes the spin and the parity of the 357-keV isomeric state ^{189m2}Bi as $13/2^+$. We assume that this state decays by the M2 transition directly to the $9/2^-$ ground state of ^{189}Bi, as in the cases of ^{191,193,195}Bi [3]. Applying a procedure described in [2], we deduced a lower limit of $T_{1/2} > 360(120)$ ns for the half-life value of the 357-keV transition.

By using the same method as described above for ^{189m2}Bi and by analysing the recoil-γ (Fig.1c) and recoil-γ-α(6450 keV) (Fig.1d) correlations a previously unknown isomeric γ–decay with the energy of $E_\gamma = 273(1)$ keV and a lower half-life limit of $T_{1/2} > 500(100)$ ns was observed on top of the α-decaying ($E_\alpha = 6450$ keV) 10^- isomeric state in ^{190}Bi. The detailed discussion of the observed results is given in [2].
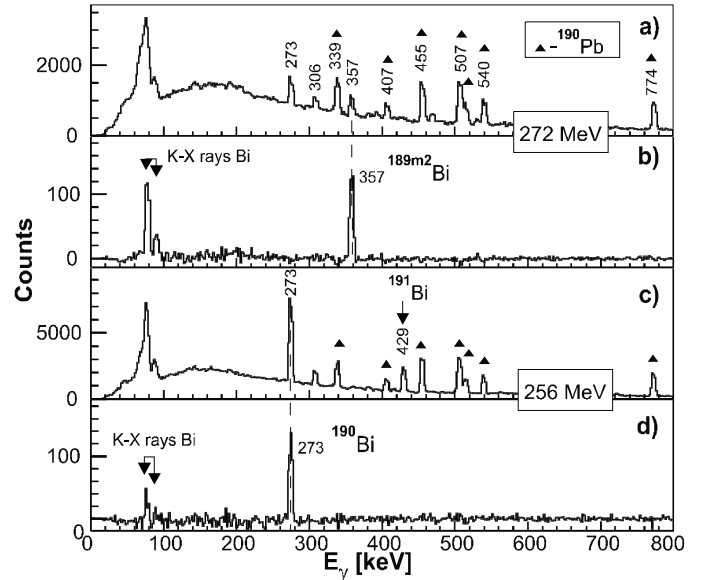

Figure 1. a) Recoil-γ coincidence spectra (time interval ΔT(EVR-γ) < 5 μs and b) background-subtracted recoil-γ-α(6672 keV) spectra for ^{189}Bi collected at the beam energy of 272.0(5) MeV; c) and d) the same as a) and b), but for ^{190}Bi, collected at the beam energy of 256.0(5) MeV. Known γ–decays of the microsecond isomeric states in ^{190}Pb [4] are marked by filled triangles.

References

[1] A.N. Andreyev et al., Eur. Phys. J. A6, 381 (1999).
[2] A.N. Andreyev et al., submitted to Eur. Phys. J. A, (2001).
[3] P. Nieminen et al., Proc. XXXV Zakopane School of Physics, Zakopane, Poland, Sep. 5-13, 2000. To be published in Acta Physica Polonica B (2001).
[4] G.D. Dracoulis, A.P. et al. Phys. Lett. B432, 37 (1998).

Direct observation of bound beta decay of bare ^{206,207}Tl at FRS-ESR

T. Ohtsubo[1,2], F. Bosch[1], H. Geissel[1,3], C. Scheidenberger[1], F. Attallah[1], K. Beckert[1], P. Beller[1],
T. Faestermann[4], B. Franzke[1], M. Hausmann[1], M. Hellström[1], P. Kienle[4], O. Klepper[1], C. Kozhuharov[1],
Yu. Litvinov[1,5], L. Maier[4], G. Münzenberg[1], F. Nolden[1], Yu. Novikov[5], T. Radon[1], V. Shishkin[1],
J. Stadlmann[3], M. Steck[1], T. Stöhlker[1], K. Sümmerer[1], H. Weick[1], M. Winkler[3]

[1] *GSI Darmstadt,* [2] *Niigata University,* [3] *JLU Gießen,* [4] *TU München,* [5] *St. Petersburg NPI*

Bound beta decay (β_b decay), the time-mirrored orbital electron capture, is a special form of β^- decay, where the electron becomes bound in an inner atomic shell (predominantly the 1s-shell) of the daughter atom. For neutral atoms the capture of an electron into an unoccupied shell has a small probabiliy because of the small overlap of the wavefunction with the nucleus. Therefore, β_b decay remains there a spurious effect only. However, when atoms get highly ionized, as, e. g., in a stellar plasma, β_b decay can become a significant decay branch. Then β^- lifetimes may alter by many orders of magnitude with respect to those of the corresponding neutral atoms, as has been proven by several experiments performed at the ESR over the last years [1,2]. The exploration of β_b decay is important for a comprehensive understanding of the creation of matter in hot stellar plasmas.

An experiment was carried out at the FRS-ESR facilities, where the β_b decay of ^{206}Tl and ^{207}Tl was *directly* observed for the first time. The mass difference between mother- and β_b daughter-atom amounts in either case to about 1.6 MeV, and the β_b decay-branch to 10-20%[3]. The ^{206}Tl and ^{207}Tl-atoms were produced by fragmentation of a ^{208}Pb primary beam in a Be target at the FRS and separated using the Bρ-ΔE-Bρ method. This technique ensured that bare Tl ions, but no hydrogen-like Pb ions were injected into the ESR. In the ESR, the ions were stored, electron-cooled, and detected via time-resolved Schottky spectroscopy. The beam noise, which is induced in pick-up electrodes, is recorded and frequency-analyzed. At the revolution frequency of each stored ion species the frequency spectrum shows lines with an area being proportional to the ion number.

Figure 1 presents the first direct observation of β_b decay. It shows time-resolved frequency spectra of the Schottky lines of stored and cooled bare ^{207}Tl^{81+} ions, together with their β_b-daughters ^{207}Pb^{81+}. The mass resolving power $m/\Delta m$ exceeds $7*10^5$, which is by far sufficient to resolve both peaks clearly. The spectra have been determined from summing-up one hundred subsequent, 64.8 milliseconds lasting measurements and covered an observation time of up to 40 minutes after injection.

Figure 2 shows the number of ions in both peaks as a function of observation time. The initial number of bare ^{207}Tl ions in the ESR was about 2000. After the cooling phase of approximately 100 seconds the intensity of the ^{207}Tl^{81+} mother nuclei decreases exponentially due to beta decay to the continuum (^{207}Pb^{82+}, not shown here), β_b decay to ^{207}Pb^{81+}, and due to charge-changing processes in the residual gas and in the electron cooler of the ESR. These unavoidable 'storage ring losses' also lead, finally, to a slow decrease of the stable ^{207}Pb^{81+} ions, whose intensity increases at the beginning due to the feeding from the decaying ^{207}Tl^{81+}.

From those spectra, together with the measured β^- decay to the continuum (β_c), a wealth of unique information will result: total

and partial β_b lifetimes, the β_b Q-value and, moreover, the ratio of bound- and continuum electron wave function, which yields the 'Fermi function'. For β^- decay, the latter has never before been probed by experiments (in contrast to β^+- and orbital electron-capture decay).

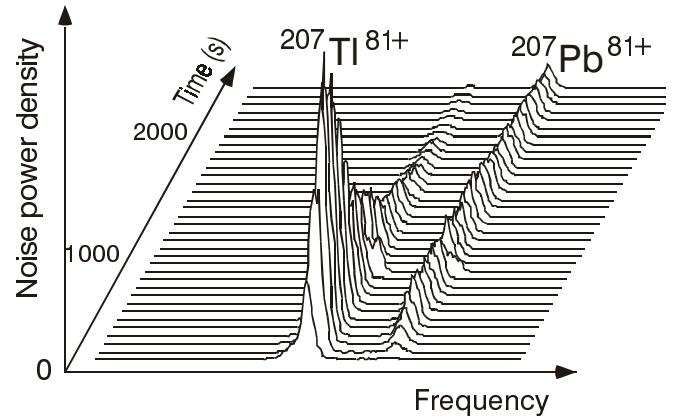Figure 1: Time-resolved frequency spectra of bare ^{207}Tl^{81+} mother and hydrogen-like ^{207}Pb^{81+} β_b-daughter ions. The noise-power is a direct measure for the number of ions.
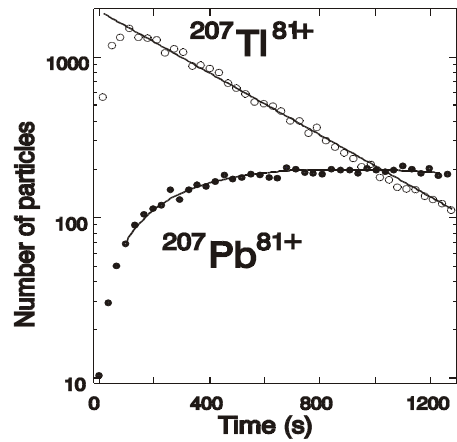

Figure 2: Number of mother (^{207}Tl^{81+}) and β_b-daughter ions (^{207}Pb^{81+}) as a function of time after injection. The first 100 seconds are needed for electron cooling of the hot fragment beams (first three data points, which have been excluded from the fit). Each data point is obtained from 32.4 seconds of observation time.

References

[1] M. Jung et al., Phys. Rev. Lett. 69, 2164 (1992).

[2] F. Bosch et al., Phys. Rev. Lett. 77, 5190 (1996).

[3] K. Takahashi et al., At. Data Nucl. Data Tables 36, 375 (1987).

Mass Measurements of Stored Exotic Nuclei

Yu.A. Litvinov[1,2], J. Stadlman[3], F. Attallah[1], K. Beckert[1], F. Bosch[1], M. Falch[4], B. Franczak[1],
B. Franzke[1], H. Geissel[1,3], M. Hausmann[1], Th. Kerscher[4], O. Klepper[1], H.-J. Kluge[1],
C. Kozhuharov[1], K.E.G. Löbner[4], G. Münzenberg[1], N. Nankov[1,3], F. Nolden[1], Yu.N. Novikov[2,5],
Z. Patyk[1], T. Radon[1], H. Schatz[1], C. Scheidenberger[1], M. Steck[1], Z. Sun[1], H. Weick[1], H. Wollnik[3]

[1] GSI, Darmstadt, Germany,   [2] State University, St. Petersburg, Russia,
[3] JLU, Giessen, Germany,   [4] LMU, München, Germany,   [5] PNPI, St. Petersburg, Russia

Exotic nuclei are produced via projectile fragmentation of different primary beams in beryllium targets placed at the entrance of the Fragment Separator (FRS). The fragments are spatially separated by the FRS, injected and stored in the Experimental Storage Ring (ESR) for direct mass measurements. Two complementary methods have been applied:

1 Schottky Mass Spectrometry (SMS)

Masses of more than 100 neutron-deficient heavy nuclides in the lead region were directly measured for the first time with a precision of roughly 100 keV in our first run with ^{209}Bi projectiles [1]. The combination of these measurements with experimental Q_α values allowed the determination of more than 60 new masses in addition [2]. The measured masses in this experiment cover a large area of proton-rich heavy nuclei up to the proton dripline.

Figure 2: Experimental shell gaps G_p for different elements (see insert) in the vicinity of the Z=82 shell [2].

magic numbers. This can be explained, for example, by nuclear shape changes along the isotopic chains.

Our second experiment with ^{209}Bi projectiles contained several improvements. The better cooler performance, stabilization of power supplies and a new data aquisition system [3] increased the resolving power by a factor of two to $m/\Delta m \approx 700000$. This allows to resolve peaks with close mass-to-charge ratios as demonstrated in Fig. 3 for
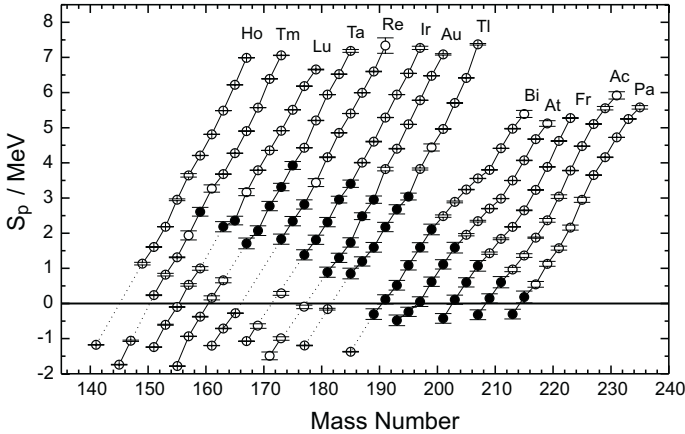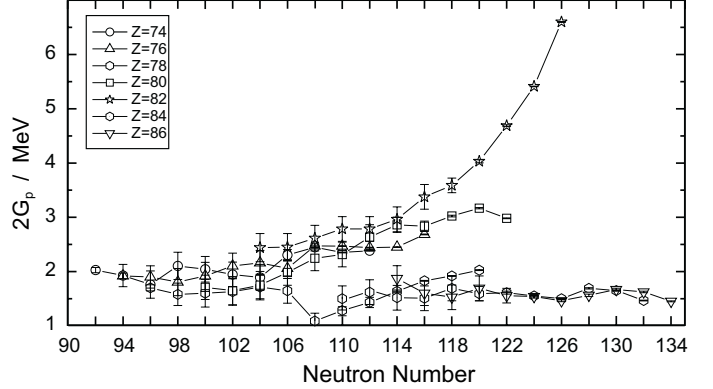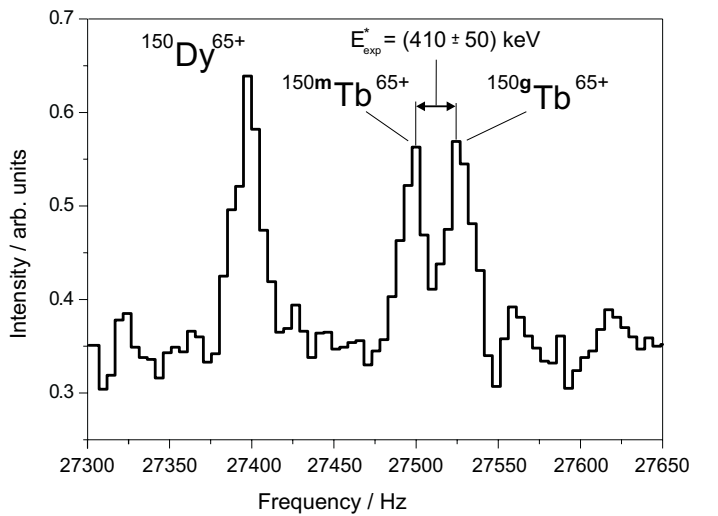

Figure 1: One-proton separation energies for odd-Z and odd-A nuclides. The full circles represent masses determined in this experiment [2].

Fig. 1 shows the one-proton separation energies for odd-Z and odd-A isotopes in the measured region. These data allowed to determine the experimental one-proton dripline for elements from bismuth to protactinium. For even-Z elements from tungsten to radium our data allow to predict reliably the two-proton dripline.

The single particle gap G_p is defined as $2G_p \equiv S_{2p}(Z, N) - S_{2p}(Z + 2, N)$, where S_{2p} is the correspondig two-proton separation energy. The G_p values for the Z=82 shell region are shown in Fig. 2. Moving away from the doubly magic ^{208}Pb nucleus towards the proton dripline the shell gap is drastically reduced, which has not been observed for other

Figure 3: Schottky spectrum representing the ground state of ^{150}Dy^{65+} ions and bare ^{150}Tb^{65+} ions in the ground and isomeric state respectively. Note that the peaks of the ground and the isomeric state of ^{150}Tb correspond to only one particle each.

the frequency peaks of the ground and isomeric states of ^{150}Tb. The excitation energy deduced from our mass measurements is in good agreement with the literature [4]. The measured mass surface of the recent experiment covers our previous measurement and adds roughly 50 new proton-rich unknown masses. Although the data analysis is still in progress we can expect a precision of the mass values of about 50 keV. Schottky Mass Spectrometry was successfully applied to nuclides with half-lives longer than 10 sec, which is needed for cooling and spectrum recording.

2 Isochronous Time of Flight Mass Spectrometry (IMS)

To extend the study to shorter half-lives the ESR was operated in an isochronous mode where the inherent velocity spread of the hot fragments is compensated by different orbit lengths [5], i.e., the revolution time is independent on the velocity spread. Therefore, precise mass measure-
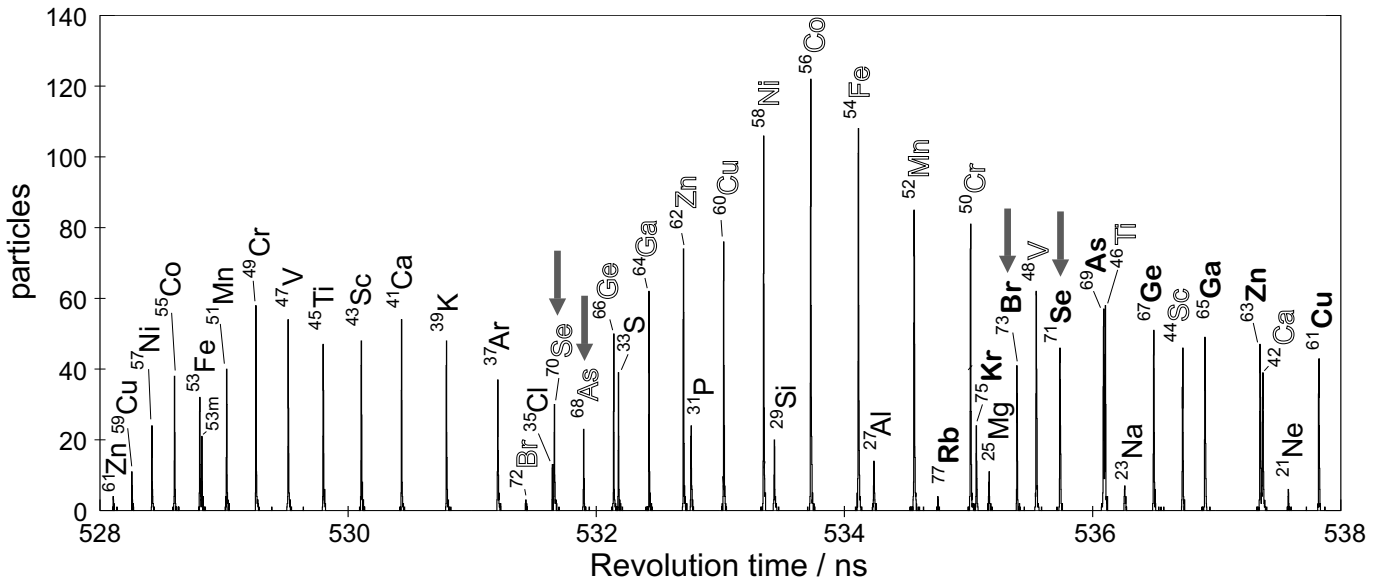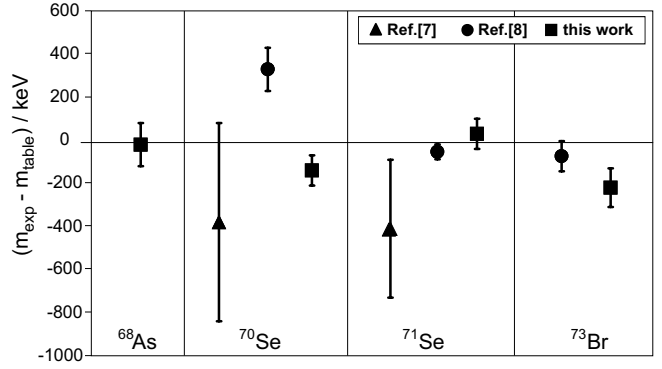
Figure 5: Comparison of mass values obtained from the isochronous TOF-measurements and other experiments [7, 8] with the table values of ref. [4]. Uncertainties of the table values are not included.

Fig. 5 shows the comparison of our results and recent measurements of ref. [7, 8] with the table values of ref. [4].

Figure 4: Revolution time spectrum of uncooled projectile fragments from a ^{84}Kr beam with an incident energy of 445.3 $A \cdot$ MeV. Groups of ions with the same isospin are marked with the same font. The arrows indicate those species which are shown in Fig. 5.

ments can be performed without beam cooling. A time-of-flight detector was used to measure the revolution times of the stored fragments within a few hundred turns in the ESR (approx. 500 ns/turn). The stored ions penetrate a thin carbon foil (17 μg/cm^2) covered with CsJ [6] (approx. 10 μg/cm^2) on each side and release secondary electrons at each turn. These electrons are detected by micro channel plates (MCPs) and the signals are recorded by a digital sampling oscilloscope. The time differences between different occurences of a particle were used to deduce its revolution time. Spectra of the revolution times were generated using the data from several injections with an identical setting. The example of such a spectrum in Fig. 4 shows only a part of the m/q - acceptance of about $\pm$ 7.5%. The mass values of ^{70,71}Se therein were unknown according to ref. [4] and the uncertainities given for ^{68}As and ^{73}Br were large. Therefore, we measured masses for these nuclides.

A mass resolving power of $m/\Delta m = 110000$ and a precision of δm $\approx$ 100 keV have been obtained. IMS is especially suited for direct mass measurements of nuclides with short half-lifes down to a few 10 μs.

References

[1] T. Radon *et al.*, Nucl. Phys. **A 677** (2000) 75

[2] Yu. N. Novikov *et al.*, submitted to Nucl. Phys. A

[3] M. Falch, Thesis, LMU München (2000)

[4] G. Audi *et al.*, Nucl. Phys. **A624** (1997) 1

[5] M. Hausmann *et al.*, NIM **A446** (2000) 569

[6] W. Thalheimer *et al.*, Cryst. Res. Technol. Vol.**34 2** (1999) 175

[7] M. Chartier *et al.*, Nucl. Phys. **A 637** (1998) 3

[8] D. Brenner, Proc. of APAC2000 to be published in Hyperfine Interaction

Fine structure in the α - decay of radium isotopes $^{212-209}$Ra

F.P. Heßberger, S. Hofmann, D. Ackermann[1]

GSI, Darmstadt, Germany, [1] also Johannes Gutenberg - Universität, Mainz, Germany

Although Ra - isotopes with mass numbers $207 \leq A \leq 212$ had been synthesized first by Valli et al. more than thirty years ago [1] little knowledge on their decay properties has been added since then. The successful application of α-γ-coincidence measurements to detect α-decay branches with low intensity in ^{214}Ra and $^{214-216}$Ac [2] motivated us also to investigate Ra-isotopes with $A \leq 212$. We therefore chose the reaction ^{204}Pb(^{12}C,xn)$^{216-x}$Ra at incident beam energies of E_{lab}= (78-137) MeV. New decay data were obtained for ^{212,211,210,209}Ra. The results are listed in table 1.

For the even - even nuclei ^{212}Ra and ^{210}Ra we observed α-decay into the first excited 2^+ - levels of the daughter nuclides. Our γ - energies of E_γ = (635.1 ± 0.2) keV for ^{212}Ra and E_γ = (574.9 ± 0.2) keV for ^{210}Ra fit well to the excitation energies of the first 2^+ - levels of ^{208}Rn (635.8 keV) and ^{206}Rn (575.3 keV) reported in literature [3].

Two weak γ - lines of E_γ = (387.0 ± 0.5) keV and E_γ = (633.7 ± 1.1) keV were attributed to the decay of ^{209}Ra. Unlike the case of the N=119 isotone ^{207}Rn, whose α-decay populates low lying states at E^* = 62.54 keV and E^* = 133 keV with relative intensities of 0.007 and 0.001, respectively, we did not observe α-γ - coincidences with E_γ < 200 keV that could be attributed to the decay of ^{209}Ra.

Altogether, six γ - lines were assigned to the decay of ^{211}Ra. While five of them fulfilled the relation $Q_\alpha + E_\gamma \approx Q_\alpha$ (gs), where Q_α and Q_α(gs) denote the Q-values for the observed transition and the ground - state transition, respectively, the 162.9 keV line delivered a considerably lower Q - value. It is, therefore, interpreted to be the transition between the E^* = 283.0 keV and E^* = 120.0 keV - levels, since it perfectly fits to the energy difference. The energy of coincident α-particles, however, is shifted by ≈20 keV as compared to α-particles coincident with E_γ = 283.0 keV. This we attribute to energy summing with conversion electrons from the transition 120 keV → 0 keV (g.s.). From the intensities of the 120 keV - line and the K_α - and K_β -lines of Rn we obtained a conversion coefficient of α = 4.5 ± 0.5 which agrees best with the value α = 6.5 expected for an M1 - transition [4]. Taking $5/2^-$ as the ground state configuration of ^{207}Rn [3], we obtain $3/2^-$ as spin and parity for the 120 keV - level. Due to the high background of x-rays from the decay by internal conversion of the 110 keV - level in ^{213}Ra, which are coincident to α - particles with energies very similar to that of α - particles coincident with the 283 keV - level in ^{211}Ra, we were not able to determine the conversion coefficient and to make a spin and parity assignment.

In the lighter N = 117 isotones ^{203}Pb and ^{205}Po two low lying levels with spins and parities $1/2^-$ and $3/2^-$ are known. While $3/2^-$ was assigned to the 120 keV level in our experiment, we did not observe a γ - line that could be attributed to the decay of a $1/2^-$ level. It should be remarked, that in our experiment we observed γ -decays from the $3/2^-$ (142.7 ± 0.5 keV) - as well as from the $1/2^-$ - level (154.5±0.5 keV) in ^{205}Po, both being populated by (^{213}Ra – α →) ^{209}Rn – α → ^{205}Po.
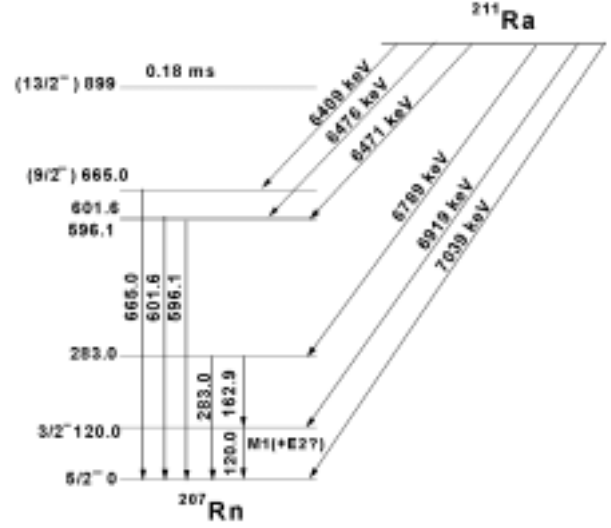

Fig. 1: Experimental decay scheme of ^{211}Ra; the energies denote the Q_α - values

Table 1: Results of α-γ - coincidence measurements for radium isotopes.

Isotope	E_α / keV	E_γ / keV
^{212}Ra	6902 ± 5	(gs)
	6269 ± 5	635.1 ± 0.2
^{211}Ra	6907 ± 5	(gs)
	6788 ± 5	120.0 ± 0.2
	(6648 ± 5)	162.9 ± 0.2
	6627 ± 5	283.0 ± 0.2
	6320 ± 10	596.1 ± 0.4
	6315 ± 10	601.6 ± 0.4
	6255 ± 5	665.0 ± 0.2
^{210}Ra	7003 ± 10	(gs)
	6447 ± 5	574.9 ± 0.2
^{209}Ra	7003 ± 10	(gs)
	6625 ± 5	387.0 ± 0.6
	6376 ± 10	633.7 ± 1.1

References:
[1] K. Valli et al. Phys. Rev 161, 1284 (1968)
[2] F.P. Heßberger et al. EPJ A 8, 521 (2000)
[3] R. Firestone et al (eds.) Table of Isotopes, 1996
[4] R.S. Hager, E.C. Seltzer Nucl. Data A4 (1968)

Fine structure in the α - decay of ^{213,214}Ac

F.P. Heßberger, S. Hofmann, D. Ackermann[1]

GSI, Darmstadt, Germany, [1] also Johannes Gutenberg - Universität, Mainz, Germany

The isotopes ^{213}Ac and ^{214}Ac were first identified in 1968 by Valli et al. [1], who reported $T_{1/2} = 0.8 \pm 0.2$ s and $E_\alpha = (7362 \pm 8)$ keV for ^{213}Ac, and $T_{1/2} = (8.2 \pm 0.2)$ s and three α-lines of $E_\alpha = 7212 \pm 5$ keV ($i_{rel} = 0.52 \pm 0.02$), 7080 ±5 keV ($i_{rel} = 0.44 \pm 0.02$), and 7000±15 keV ($i_{rel} = 0.04 \pm 0.01$) for ^{214}Ac. In a recent experiment [2] new results on the decay of ^{214}Ac were obtained by means of α-γ- coincidence measurements, but due to low count rates some of the assignments had to be regarded as tentative. To study its decay in more detail and also to search for fine structure in the α-decay of ^{213}Ac we produced them by the reaction ^{209}Bi(^{12}C, xn)^{213,214}Ac (x=8,7). The nuclides were separated from the projectile beam in-flight by SHIP and implanted into a 16-strip-Si-detector, where their α-decay was measured in coincidence with γ-rays registered with a high purity Ge-detector mounted closely behind the Si- detector.

Two γ - lines of $E_\gamma = (341.6 \pm 0.4)$ keV and $E_\gamma = (608.8 \pm 0.5)$ keV were assigned to the decay of ^{213}Ac; the energies of the coincident α-particles are (7022±10) keV and (6767±10) keV. The result for ^{214}Ac was more complex; besides coincidences characterized by $E_\gamma + Q_\alpha = Q_\alpha(gs) \pm 10$ keV (Q_α, $Q_\alpha(gs)$ are the Q-values of the observed and of the ground-state (gs) transition, resp.) and $\Delta E_\alpha(FWHM) < 30$ keV, we also observed those having $E_\gamma + Q_\alpha < Q_\alpha(gs)$ and/or $\Delta E_\alpha(FWHM) > 30$ keV. The first group is assigned to γ-dcays into the gs or low lying levels. (Summing with conversion electrons (CE) from those states will shift the α-energy close to the value of the gs transition, while the line width is not effected significantly, as shown for ^{212}Fr α-γ decays into the 23.5 keV - level in ^{208}At, followed by L - conversion to the gs.)

The second group is interpreted as transitions between excited states. A preliminary decay scheme based on these results is shown in fig 1. The tentative assignment of the γ-lines reported in [2] was confirmed and some weaker transitions, not indicated so far, were observed. However, these results led to new questions: especially the assignment of two strong γ-transitions $E_\gamma = 224.8$ keV and $E_\gamma = 162.5$ keV still causes some problems. Since $\Delta E = (363.8-139.0)$ keV = 224.8 keV the first line may be attributed to the transition between these two levels, which is supported by the energy distribution of the coincident α-particles. About 62% have a mean energy $E_\alpha = 6868$ keV (i.e. close to that coincident to $E_\gamma = 363.8$ keV) and 18% $E_\alpha = 6909$ keV, which can be understood as due to summing with K - CE from decay of the 139.0 keV - level. Yet, 20% have $E_\alpha = 6989$ keV. The intensity is too high for summing with L - CE since for an M1 - transition at $\Delta E = 139$ keV, $i(K)/i(L) \approx 2.4$ is expected. We thus tentatively assume a level at $E = 224.8$ keV, having accidentally (within our experimental accuracy) the same energy as the 363.8 keV → 139.0 keV - transition. This assumption is corrobated by the 162.5 keV - line, which is close to $\Delta E = (224.8-62.6)$ keV. The energy distribution of the α -particles coincident to this line does not support a transition to the ground state, but is very similar to that of those coincident to the E = 146.5 keV - line, which is interpreted as the transition 209.3 keV → 62.6 keV.

References:

[1] K. Valli et al. Phys. Rev. 167, 1094 (1968)
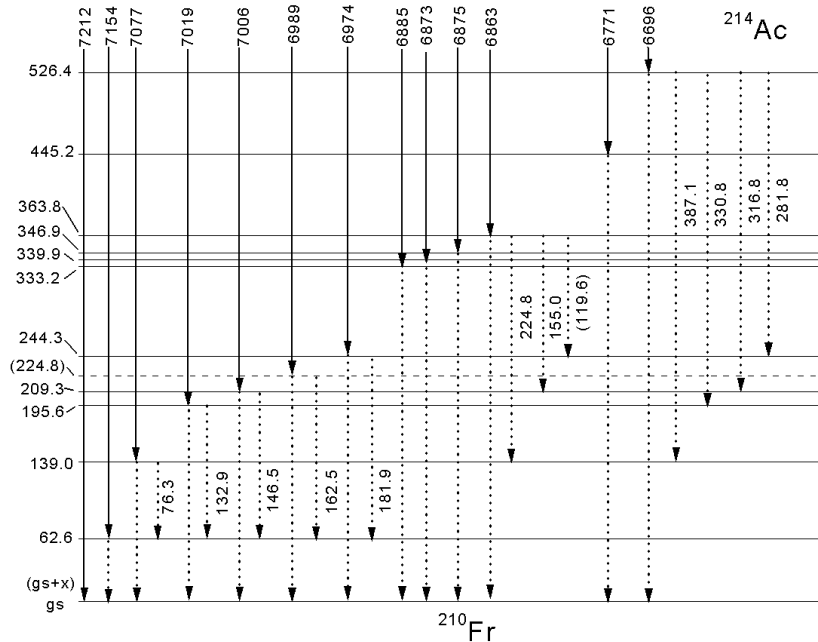[2] F.P.Heßberger et al. EPJ A 8, 521 (2000)

Fig. 1: Decay scheme suggested for ^{214}Ac; full lines: α-decay; dashed lines: observed γ-decays (energies for gs transitions are omitted)

Deeply Bound *1s* and *2p* Pionic States and the *s*-Wave Part of the Pion-Nucleus Interaction

H. Geissel[1], H. Gilg[2], A. Gillitzer[3], R. S. Hayano[4], S. Hirenzaki[5], K. Itahashi[6], M. Iwasaki[6], P. Kienle[2], M. Münch[2], G. Münzenberg[1], K. Suzuki[4], W. Schott[2], D. Tomono[6], H. Weick[1], T. Yoneyama[6], T. Yamazaki[7]

[1]GSI Darmstadt, [2]Technische Universität München, [3]Forschungszentrum Jülich, [4]University of Tokyo, [5]Nara Women's University, [6]Tokyo Institute of Technology, [7]RIKEN
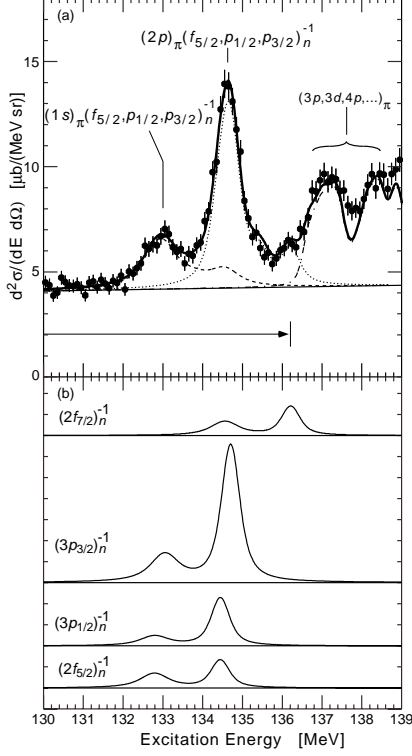
Figure 1: Measured excitation energy spectrum for the ^{206}Pb(d,^{3}He) reaction ($T_d = 600$ MeV) in the region of the bound pionic states. In a fit (fitting region indicated by the arrow) $(1s)_\pi$ and $(2p)_\pi$ peak are decomposed into the contributing neutron hole configurations of which the most important are $2f_{5/2}$, $3p_{1/2}$ and $3p_{3/2}$.

Figure 2: Binding energy and width of the $(1s)_\pi$ state in ^{205}Pb related to the real ($V(0)$) and imaginary ($W(0)$) part of the *s* - wave potential in the center of the nucleus. The *p* - wave potential is taken from a parameter set given by Seki and Masutani [5]

After the discovery of the deeply bound $(1s)_\pi$ and $(2p)_\pi$ states in ^{207}Pb in the ^{208}Pb(d,^{3}He) reaction [1] and the determination of the real and imaginary *s*-wave-potential parameters b_0 and ImB_0 from the $(2p)_\pi$ binding energy and width [2, 3], a new experiment on the ^{206}Pb(d,^{3}He) reaction was performed at the Fragment Separator (FRS). The better suited neutron shell structure of ^{206}Pb compared to ^{208}Pb and an improved energy resolution allowed for a clear separation of the $(1s)_\pi$ component from the dominant $(2p)_\pi$ peak in the excitation spectrum [4], which was not achieved in the ^{208}Pb(d,^{3}He) experiment. Accordingly the binding energy and width of the $(2p)_\pi$ state (B_{2p}, Γ_{2p}) and especially of the $(1s)_\pi$ state (B_{1s}, Γ_{1s}) can be determined with significantly higher precision.

Decomposing the excitation energy spectrum into $(1s)_\pi$ and $(2p)_\pi$ components coupled to different neutron hole contributions (Figure 1) the values $B_{1s} = 6.768 \pm 0.044$ (stat.) ± 0.041 (syst.) MeV, $\Gamma_{1s} = 0.778^{+150}_{-130}$ (stat.) $\pm$
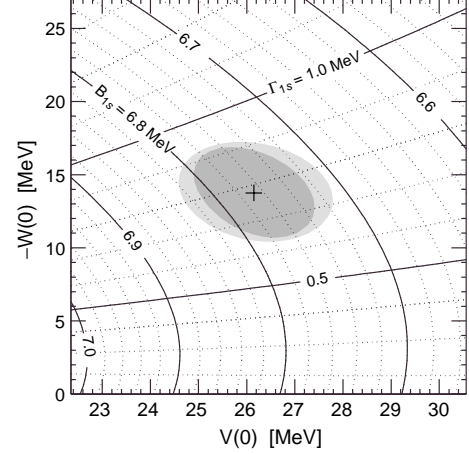
0.055 (syst.) MeV, $B_{2p} = 5.110 \pm 0.015$ (stat.) ± 0.042 (syst.) MeV and $\Gamma_{2p} = 0.371 \pm 0.037$ (stat.) ± 0.048 (syst.) MeV were obtained.

These quantities were used to determine the pion-nucleus *s* - wave optical potential. The most precise values for the real and imaginary part ($V(0) = 26.1^{+1.7}_{-1.5}$ MeV, $W(0) = -13.8^{+3.4}_{-3.5}$ MeV) were deduced from B_{1s} and Γ_{1s} (Figure 2). The 1s state has a larger sensitivity, since the pionic 1s wave function has larger overlap with the nuclear density distribution than the 2p wave function, and since the 1s binding energy and width are almost exclusively determined by the *s* -wave potential parameters. With the assertion that the isovector term of the π^--nucleus interaction $b_1^\star$ is modified in the medium and that the isoscalar part is induced by double scattering mainly, one can derive from $V(0) = 26.1$ MeV for ^{205}Pb that $b_1^\star \simeq -0.125 m_\pi^{-1}$. This also indicates a reduction of the quark condensate to 72%.

References

[1] T. Yamazaki *et al.*, Z. Phys. **A355** (1996) 219, H. Gilg *et al.*, GSI Scientific Report 1996, p. 40

[2] T. Yamazaki *et al.*, Phys. Lett. B **418** (1998) 246

[3] H. Gilg *et al.*, Phys. Rev. C **62**, 025201 (2000) K. Itahashi *et al.*, Phys. Rev. C **62**, 025202 (2000)

[4] H. Geissel *et al.*, GSI Scientific Report 1999, p. 31

[5] R. Seki, K. Masutani, Phys. Rev. C **27** (1983) 2799

# Excitation and Fragment-Neutron Correlations of Halo Nuclei [B,G]

D. Aleksandrov[1], T. Aumann[2], L. Axelsson[3], T. Baumann[2], M.J.G. Borge[4], D. Cortina-Gil[2], L.V. Chulkov[1,2],
W. Dostal[5], B. Eberlein[5,2], Th.W. Elze[6], H. Emling[2], C. Forssén[3], H. Geissel[2], A. Grünschloß[6], M. Hellström[2],
B. Jonson[3], J.V. Kratz[5], R. Kulessa[7], Y. Leifels[2], A. Leistenschneider[6], K. Markenroth[3], M. Meister[3,8], I. Mukha[1,8],
G. Münzenberg[2], T. Nilsson[3], G. Nyman[3], M. Pfützner[2], A. Richter[8], K. Riisager[9], C. Scheidenberger[2], G. Schrieder[8],
H. Simon[8], O. Tengblad[4], M.V. Zhukov[3]

[1]Kurchatov Institute, Moscow, [2]GSI Darmstadt, [3]CTH Göteborg, [4]CSIC Madrid, [5]Univ. Mainz, [6]Univ. Frankfurt,
[7]Univ. Kraków, [8]TU Darmstadt, [9]Univ. Aarhus,

Dissociation of ^{8}He and ^{14}Be in carbon and lead targets has been studied in kinematically complete experiments. The data allow to deduce invariant mass spectra, angular distributions in the one neutron knock-out channel as well as inelastic scattering in the 2n decay channels.

The invariant mass spectrum in the inelastic channel ^{6}He+n+n shows a broad distribution extending up to about 3.5 MeV. This may be interpreted either (i) as a single broad 1^- resonance or (ii) as a relatively narrow 2^+ state and a broad peak from higher excited 1^- state.

Figure 1: Differential cross section for inelastic scattering of ^{8}He on two different targets. C target (top): experimental data are compared with DWBA calculations for dipole (dotted line) and quadrupole (dashed line) excitations. Pb target (bottom): the contribution from the electromagnetic dissociation is shown as dashed line while the nuclear diffractive dissociation is displayed as dotted lines. The calculations where performed in eikonal DWBA and result in the solid line as sum of the two processes.
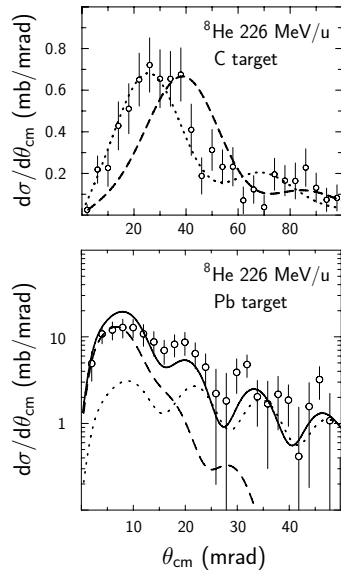
The dominance of dipole transitions can be seen in Figure 1 (top) where the experimental angular distribution for ^{8}He inelastic scattering on a carbon target [1] is shown in comparison with DWBA calculations. The differential cross section obtained for ^{8}He inelastic scattering from a lead target shown in Fig. 1 (bottom) exhibits Coulomb-nuclear interferences, thus confirming the $J^\pi = 1^-$ assignment to a broad peak in the ^{8}He invariant-mass spectrum.

Table 1 presents partial cross sections for the ^{8}He fragmentation on carbon and lead targets. In both cases, neutron knock-out is the dominating reaction channel. It becomes comparable in magnitude with the inelastic scattering in case of the ^{208}Pb target. For the carbon target, the difference of the ^{8}He and ^{4}He interaction cross sections exceeds the sum $\sigma_{in} + \sigma_{-1n} + \sigma_{-2n}$ in ^{8}He by about 100 mb. This excess is due to the breakup into $\alpha+4$n and is likely a sign of the five-body character of ^{8}He.

For the lead target, the difference of the ^{8}He and ^{4}He interaction cross sections is smaller than the sum $\sigma_{in} + \sigma_{-1n} + \sigma_{-2n}$. The Coulomb dissociation cross section can be calculated from this difference by taking into account the missing contribution of about 250 mb from the breakup into $\alpha+4$n. An independent method based on DWBA calculations and a normalisation to the experimental angular distribution at forward angles gave the same result. The contribution of electromagnetic dissociation is then 160 mb which leads to a B(E1) value equal to $0.46\,e^2fm^2$ below 7 MeV excitation energy.

Table 1: Extracted contributions of nuclear (N) and electromagnetic (C) processes to the fragmentation cross sections of ^{8}He on lead and on carbon targets. Here σ_{in} denotes cross sections for inelastic scattering, whereas σ_{-1n} corresponds to one-neutron knock-out.

Target	σ_{in}^N (mb)	σ_{in}^C (mb)	σ_{-1n}^N (mb)	σ_{-1n}^C (mb)
Lead	80 ± 12	160 ± 25	322 ± 37	6 ± 97
Carbon	32 ± 5		129 ± 15	

The structure of the unbound ^{13}Be is currently poorly understood. The ^{12}Be-n relative energy spectrum shown in Figure 2 and obtained in a one-neutron knockout reaction of ^{14}Be on a carbon target, reveals interesting structures. The angular distributions analysed as explained in [2], but gated on different bins in the relative energy spectrum show isotropy (bottom,left) and asymmetry (bottom,right) as expected for adopted s- and p- wave resonances at about 250 keV and 1.2 MeV, respectively.

Figure 2: (Top) The relative energy spectrum between ^{12}Be fragments and neutrons. The solid line represents a fit to the data taking s (dotted), p (dashed) and d (dashed dotted) contributions into account. (Bottom) angular distributions gated on the relative energy as indicated by the shaded areas. The solid lines are fits with 2nd order polynomials to guide the eye.
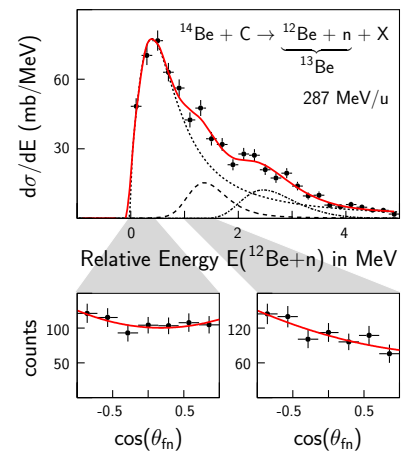
The asymmetric distribution stems hereby from the interference of two overlapping states with different parity. As the groundstate shows the typical behaviour of an s-intruder state, the interfering first excited state should be a p-state. This allows a tentative assignment of $(1s_{1/2})$, $(0p_{1/2})$ and $(0d_{5/2})$ for the groundstate and the first two excited states of ^{13}Be.

References

[1] K. Markenroth et al., Nucl. Phys. **A679** (2001) 462
[2] H. Simon et al., Phys. Rev. Lett. **83** (1999) 469

Nuclear Matter Distributions of Neutron-Rich Li-Isotopes from Elastic Proton Scattering in Inverse Kinematics

A.V. Dobrovolsky[1,2], G.D. Alkhazov[2], M.N. Andronenko[2], A. Bauchet[1], P. Egelhof[1],
S. Fritz[1], G.E. Gavrilov[2], H. Geissel[1], C. Gross[1], A.V. Khanzadeev[2], G.A. Korolev[2], G. Kraus[1],
A.A. Lobodenko[2], G. Münzenberg[1], M. Mutterer[3], S.R. Neumaier[1], T. Schäfer[1], C. Scheidenberger[1],
D.M. Seliverstov[2], T. Suzuki[1], N.A. Timofeev[2], A.A. Vorobyov[2] and V.I. Yatsoura[2]

[1] GSI Darmstadt, [2] PNPI Gatchina, [3] TU Darmstadt

The method of proton elastic scattering at intermediate energies, which was already proven for the neutron-rich helium isotopes ^{6,8}He [1],[2] to be well suited for obtaining accurate and detailed information on nuclear matter distributions of halo nuclei, was recently applied for the investigation of the lithium isotopes ^{6,8,9,11}Li. Absolute differential cross sections $d\sigma/dt$ for small-angle Li-p elastic scattering were determined by an inverse-kinematics measurement using secondary Li-beams with $E \approx 0.7$ GeV/u from the SIS-FRS, and gaseous hydrogen as the proton target. The hydrogen filled ionization chamber IKAR served simultaneously as target and detector for recoil protons. Projectile scattering angles were measured precisely with multi-wire tracking detectors. Furthermore, a magnetic-rigidity analysis of the scattered particles was performed with the aid of the ALADIN magnet and a position sensitive scintillator wall behind for the separation of neutron break-up channels. For this purpose the entire experimental setup was installed at the Cave B.

The data analysis has fairly progressed within the year 2000. The (still preliminary) differential cross sections $d\sigma/dt$ for p^{9,11}Li scattering are displayed in Fig. 1 together with the cross section for p^{6}Li scattering, the results of which were discussed already in the previous GSI annual report 1999.

For establishing the nuclear density distributions from the measured cross sections, the Glauber multiple scattering theory was applied. Calculations were performed using the basic Glauber formalism for proton-nucleus elastic scattering, and taking experimental data on the elementary proton-proton and proton-neutron scattering amplitudes as input. In the present analysis two different parametrizations for modelling the nuclear density distribution were used for the Glauber calculations, and the parameters were varied in order to obtain a best fit to the experimental cross sections. Both parametrizations applied assume the nuclei involved to consist of a core and two valence neutrons. A Gaussian distribution for the core, and either a Gaussian (GG) or a 1p-shell harmonic
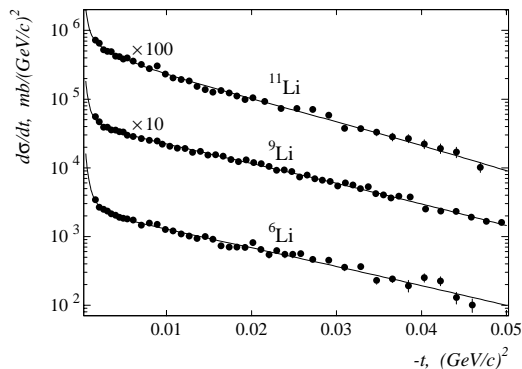

Figure 1. Absolute differential cross sections $d\sigma/dt$ versus the four momentum transfer squared t for p^{6,9,11}Li elastic scattering obtained from the present experiment. Full lines are the result of fits to the data performed on the basis of the Glauber multiple scattering theory.
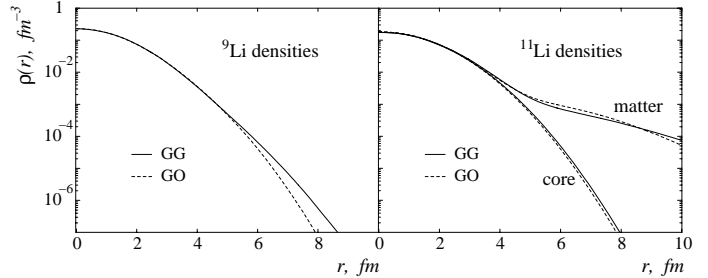

Figure 2. The nuclear matter and nuclear core density distributions $\rho(r)$ of ^{11}Li deduced from the present experimental data are compared with the nuclear matter density distribution of ^{9}Li. Labels denote different parametrizations of phenomenological density distributions used in the analysis (see text).

oscillator-type density (GO) for the valence neutrons were used (for details see ref.[1]). The experimental data are comparably well described with both density parametrizations, with a reduced χ^2 around unity. Solid lines in Fig. 1 show the GG case as an example.

The nuclear matter distributions of ^{11}Li and ^{9}Li deduced from the present data are displayed in Fig. 2. The radii obtained for the total matter, the core, and the halo distributions for ^{9,11}Li are given in Table 1 in comparison with those of ^{6,8}He from the previous experiment [1],[2]. It is obvious from the data that the matter distribution of ^{11}Li exhibits the by far most pronounced halo structure compared to all the other nuclei investigated, including ^{6}He and ^{8}He. This is also reflected in the deduced nuclear matter radius $R_m = 3.62$ (14) fm and the halo radius $R_h = 6.54$ (38) fm, the latter being more than twice as large as in ^{6}He and ^{8}He. A comparison of the nuclear matter and core distributions of ^{11}Li with the matter distribution deduced for ^{9}Li, and the corresponding radii (Table 1), supports the generally accepted picture of ^{11}Li to consist of a ^{9}Li core and a two-neutron halo.

Table 1: Summary of nuclear matter radii deduced for the helium isotopes ^{6,8}He [1],[2] and for the lithium isotopes ^{9,11}Li from the present experiment (please note that the results on the lithium isotopes are still preliminary). R_m denotes the total rms matter radius, R_c the core radius, and R_h the halo radius. The errors given include statistical and systematical uncertainties.

nucleus	R_m	R_c	R_h
^{6}He	2.30 (7)	1.88 (12)	2.97 (26)
^{8}He	2.45 (7)	1.55 (15)	3.08 (10)
^{9}Li	2.43 (7)	2.21 (10)	3.10 (28)
^{11}Li	3.62 (14)	2.55 (12)	6.54 (38)

References

[1] G.D. Alkhazov et al., Phys. Rev. Lett. 78 (1997) 2313

[2] S.R. Neumaier et al., Nucl.Phys. A (2001), to be published

Coulomb Breakup of ^{15}C and ^{17}C [B,G]

U. Datta Pramanik[1], T. Aumann[1], K. Boretzky[2], D. Cortina-Gil[1], Th.W. Elze[3], H. Emling[1], H. Geissel[1], A. Grünschloß[3],
M. Hellström[1], S. Ilievski[3], N. Iwasa[1], J.V. Kratz[2], R. Kulessa[4], Y. Leifels[1], A. Leistenschneider[3], E. Lubkiewicz[4],
G. Münzenberg[1], P. Reiter[5], C. Scheidenberger[2], Ch. Schlegel[1], H. Simon[6], K. Sümmerer[1], E. Wajda[4], W. Walus[4]

(LAND-FRS Collaboration)

[1]GSI Darmstadt, [2]Univ. Mainz, [3]Univ. Frankfurt, [4]Univ. Kraków, [5]LMU München, [6]TU Darmstadt

Coulomb breakup of secondary beams of unstable nuclei at intermediate energies has developed into a standard spectroscopic tool in exploring properties of weakly bound nuclei. Here, this method has been applied to a study of ^{15}C and ^{17}C isotopes which have very small neutron separation energies of 1.2 and 0.73 MeV, respectively.

Radioactive beams of ^{15,17}C were produced in a fragmentation reaction of a primary ^{40}Ar beam, delivered by the synchrotron SIS at GSI, Darmstadt, and were subsequently separated in flight by the FRS. The incoming beam and fragments were identified utilizing energy-loss and time-of-flight measurements together with the known magnetic rigidity. Neutrons and γ-rays were detected by the LAND and Crystal Ball spectrometers, respectively. From the measured momenta of all decay products of the projectile after inelastic scattering followed by breakup, the excitation energy of the nucleus was determined. The Coulomb dissociation cross sections with the Pb (1.8 g/cm^2) target were obtained after subtracting nuclear contributions determined from the data with a C (0.573 g/cm^2) target.

By comparing measured differential cross sections $d\sigma/dE^*$ (excitation energy E^*) for electromagnetic excitation with calculated cross sections (see below) one can deduce information on the ground state structure. The Coulomb breakup cross section can be written [1]:

$$\frac{d\sigma}{dE^*} = (\frac{16\pi^3}{9\hbar c})N_{E1}(E^*)\sum_m |< q \mid (Ze/A)rY_m^1 \mid \psi(r) >|^2 .$$

$N_{E1}(E^*)$ represents the number of equivalent dipole photons of the target Coulomb field, computed in a semiclassical approximation, $\psi(r)$ represents the ground state single particle wave function of the neutron and $< q \mid$ describes the wavefunction of the neutron in the continuum.

In the case of ^{15}C with the known g.s. spin I$^\pi$ = $1/2^+$, the experimental data show that Coulomb breakup populates predominatly the ground state of ^{14}C, a small branch of about 10 % feeding excited states at 6 - 7 MeV is observed in addition. A comparision between our measured $d\sigma/dE^*$ for this isotope with the fragments in its ground state and the calculated one, delivers a spectroscopic factor (0.72) for a ℓ=0 neutron which is consistent with an earlier reported value [2].

The ground state spin of ^{17}C is not fully established experimentally. Our experimental data for Coulomb break up of ^{17}C show that most of the cross section yields the ^{16}C core in its first excited state, I$^\pi$= 2$^+$, and an excited state at an excitation energy around 3 MeV. Only a small part of the cross section leaves the core in its ground state. Fig. 1 (top) shows the sum energy spectra of the γ decay from ^{16}C fragments and indicates the relative
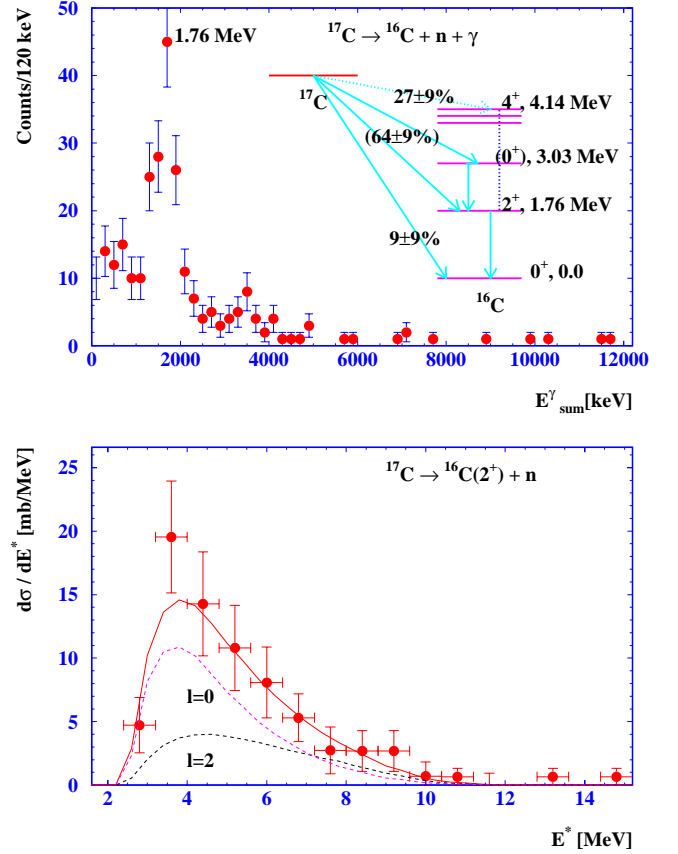

Fig. 1: Sum energy of γ decay transitions (top). Differential Coulomb dissociation cross section (bottom).

partial cross sections for the population of different core states. The lower part of the Fig. 1 shows $d\sigma/dE^*$ for electromagnetic excitation of ^{17}C in coincidence with the 1.766 MeV γ transition ^{16}C($2^+ \to 0^+$) without acceptance and efficiency corrections for the neutron detector. These corrections, however, are taken into account in the cross sections calculated according to equ. (1). A proper choice of relative contributions from $\ell = 0$ and $\ell = 2$ neutrons forming the ^{17}C g.s. wave function, as shown Fig 1, can reproduce well the data. Thus, ^{16}C(2^+) $\bigotimes \nu_{s,d}$ is the predominant g.s. configuration and one can rule out a $1/2^+$ ground state spin of ^{17}C. The major part of our results is in agreement with those from a different method, i.e. obtained from a knockout reaction [3].

References

[1] T. Nakamura et al., *Phys. Rev. Lett.* **83** (1999) 1112.

[2] J.D. Goss et al., *Phys. Rev.* C **8** (1973) 514.

[3] V. Maddalena et. al., *Phys. Rev.* C **63** (2001) 024613.

Nuclear Halo Structure Studies via High-Energy Break-up Reactions

D. Cortina-Gil[1,2], J. Fernandez-Vazquez[1], K. Markenroth[3], T. Aumann[2], T. Baumann[4], J. Benlliure[1], K. Boretzky[2], M.J.G. Borge[5], L. Chulkov[2,6], U. Datta-Pramanik[2], Ch. Forssen[3], Luis M. Fraile[5], H. Geissel[2], J. Gerl[2], F. Hammache[2], V. Hansper[7], K. Ithashi[8], M. Ivanov[2], R. Janik[9], B. Jonson[3], T. Kato[10], K. Kimura[11], S. Mandal[2], M. Meister[3], M. Mocko[9], G. Münzenberg[2], T. Ohtsubo[2,10], S. Ohya[10] T. Okuda[12], A. Ozawa[13], Y. Prezado[5], V. Pribora[6], K. Riisager[7], G. Schneider[14], H. Scheit[15], G. Schrieder[16], M. Sekiguchi[12], B. Sitar[9], A. Stolz[14], P. Strmen[9], K. Sümmerer[2], T. Suzuki[9], X. Szarka[9], I. Tanihata[13], S. Wan[2], H. Weick[2], Y. Yamaguchi[10]

[1]Universidad de Santiago de Compostela, [2]GSI, [3]CTH Göteborg, [4]MSU, [5]Instituto de Estructura de la Materia, [6]Kurchatov Institute, [7]Aarhus Universitet, [8]Tokyo Institute of Technology, [9]Comenius University, [10]Niigata University, [11]Nagasaki Institute of Applied Science, [12]Tohoku University, [13]RIKEN, [14]TU München, [15]MPI, [16]TU Darmstadt

The nuclear halo structure can be efficiently investigated via high-energy breakup reactions. Partial and differential break-up cross section measurements for the removal of valence nucleons and momentum measurements are spectroscopic methods successfully applied at high-energy fragmentation facilities. A narrow momentum distribution of the core fragments can be a clear signature for new halo candidates [1, 2, 3]. In recent experiments at the FRS we measured the momentum distributions of neutron-rich oxygen isotopes isotopes produced via fragmentation of ^{40}Ar projectiles. The fragments were unambiguously identified by magnetic rigidity, time-of-flight and energy-deposition measurements in front of the breakup target placed at the central focal plane of the FRS. Momentum distributions of the secondary fragments after removal of one neutron are shown in fig. 1.
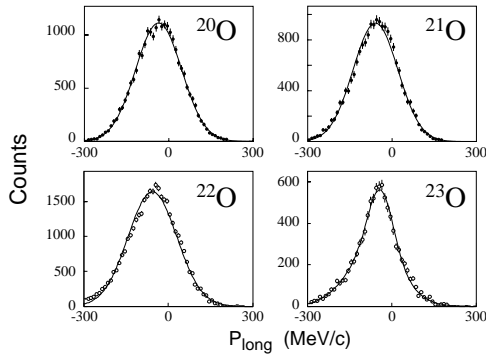

Figure 1: Measured momentum distributions of oxygen isotopes after one-neutron removal reaction in a carbon breakup target placed at the central focal plane of the FRS. The preliminary fwhm values of the distributions are ^{20}O $(192 \pm 5$ MeV/c), ^{21}O $(187 \pm 9$ MeV/c), ^{22}O $(203 \pm 14$ MeV/c) ^{23}O $(130 \pm 8$ MeV/c).

The narrow momentum distribution of the valence neutron in ^{23}O reflects a clear shell structure in accordance to the observation in ref.[4]. From the shape of the measured longitudinal momentum distribution the orbital angular momentum of the removed nucleon can be determined and from the removal cross section the spectroscopic factors. These powerful spectroscopic tools were extended by γ-ray detection to identify the final states of the core fragments after the removal reaction. The gamma detector consisted of an array of 32 NaI units located 80 cm behind of the breakup target (total efficiency (ϵ)= 3 % and energy reso-

lution (ΔE/E)= 12% for E_γ=429 keV).

The method is illustrated by a test measurement of ^{8}B, performed in the beginning of this experimental campaign. In this part, the ^{8}B beam was produced by fragmentation of a primary beam of ^{12}C at 1 GeV/nucleon. The nuclear structure of ^{8}B was studied via one-proton removal reaction in lead and carbon breakup targets and the measured momentum distributions were recorded in coincidence with γ-ray spectroscopy. The corresponding one-proton removal cross section are: σ_{-1p}(C) = (94 $\pm$ 9) mb and σ_{-1p}(Pb) = (662 $\pm$ 60) mb both in excellent agreement with our earlier measurements [5].

The contributions from the ground and excited state to the ^{7}Be momentum distribution after the p-removal in the carbon target are shown in fig.2. It is clearly seen that the ground-state transition dominates the measured momentum distribution.

The data analysis for the oxygen isotopes is still in progress, however, the preliminary results show that we can extract the above mentioned spectroscopic information. In future, we will extend the measurements to heavier elements and will also use a hydrogen breakup target in combination with an improved γ-setup.
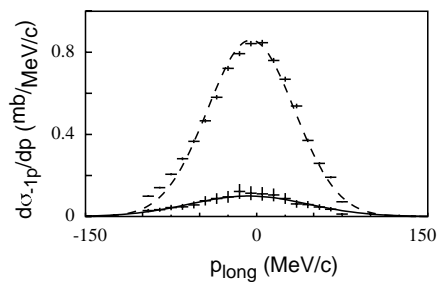

Figure 2: The measured momentum distribution of ^{7}Be. The separate contributions for the transition in the ground-state (dashed line) and first excited state (full line) after the p-removal in the lead target are shown.

References

[1] W. Schwab et al., Z. Phys. A 350 (1995) 283.
[2] T. Baumann et al., Phys. Lett. B 439 (1998) 256.
[3] M.H. Smedberg et al., Phys. Lett. B 452 (1999) 1.
[4] A. Ozawa et al., Phys. Rev. Lett. 84 (2000) 5493
[5] D. Cortina-Gil et al, Eur. Phys. J. A 10 (2001)49

Model calculations of a two-step reaction scheme for the production of the neutron-rich secondary beams

J. Benlliure, K. Helariutta, M.V. Ricciardi, K.-H. Schmidt

Actually, the design of more powerful next-generation secondary-beam facilities is being intensively discussed. The main challenge is the production of neutron-rich isotopes, because the neutron-drip line has only been reached for the lightest elements. The traditional way for producing neutron-rich nuclei is fission of actinides. Another approach introduced recently, based on cold fragmentation [1], has successfully been used to produce a number of new neutron-rich isotopes. A new idea is to combine these two methods in a two-step reaction scheme. Medium-mass neutron-rich isotopes are produced with high intensities as fission fragments. They are used as projectiles in a second step to produce even more neutron-rich nuclei by cold fragmentation. This idea might be realised in an-flight facility by consecutive reactions in a thick target, while the application in an ISOL-based facility needs post acceleration to sufficiently high energies to allow for fragmentation in a second target.

In our recent work [2], we studied the feasibility of this two-step reaction scheme by calculating the relevant cross sections and the beam intensities to be obtained. We concentrated our studies on the second step of this approach, cold fragmentation of projectiles far from stability, since there are no experimental data available for the fragmentation of exotic, very neutron-rich projectiles. Two types of codes were used, EPAX [3], the semi-empirical parameterisation of fragmentation cross sections and COFRA [4,1], a modern analytical version of the abrasion-ablation nuclear reaction model. In figure 1, the cross sections from fragmentation of ^{132}Sn as predicted by the two codes are compared. While the EPAX code extrapolates the production cross sections, measured in fragmentation of the available stable projectiles, the nuclear-reaction code takes into account the variation of the nuclear properties as a function of neutron excess. Most important is an enhanced neutron evaporation caused by the low neutron-separation energies of the extremely neutron-rich fragments. This leads to considerably lower cross sections if compared to EPAX.

According to the COFRA calculations, the direct production by fission of ^{238}U prevail in most cases. The two-step scenario might only become advantageous in the production of extremely neutron-rich isotopes. The situation changes appreciably if we consider the available secondary-beam intensities including extraction, ionisation and re-acceleration in an ISOL-type facility. Here, the two-step reaction scenario can be useful by profiting from very high secondary-beam intensities to be obtained for specific neutron-rich nuclides. Extracting an abundant and long-lived neutron-rich nuclide like ^{132}Sn from the ISOL source and fragmenting it, one can reach those isotopes that have low ISOL efficiencies due to their short half lives or difficulties in the extraction from the source [5].

We conclude that the predictions of EPAX for the production of very neutron-rich nuclides by fragmentation of non-stable neutron-rich projectiles seem to be far too optimistic. The two-step reaction scheme studied might be advantageous in specific cases.
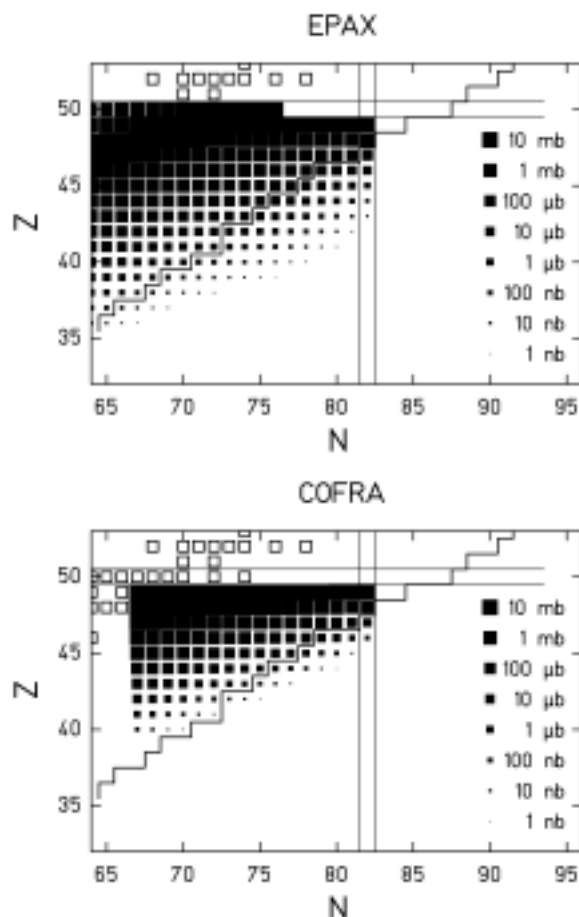

Figure 1. Predicted cross sections for the cold-fragmentation of ^{132}Sn in beryllium target from the empirical systematics EPAX and the nuclear-reaction code COFRA on a chart of the nuclides.

References

[1] J. Benlliure , K.-H. Schmidt, D. Cortina-Gil, T. Enqvist, F. Farget, A. Heinz, A. R. Junghans, J. Pereira, J. Taieb, Nucl. Phys. **A 660** (1999) 87.

[2] J. Benlliure, K. Helariutta, M.V. Ricciardi, K.-H. Schmidt, GSI-Preprint-00-41, November 2000.

[3] K. Sümmerer and B. Blank, Phys. Rev. **C 61** (2000) 034607.

[4] J.-J. Gaimard and K.-H. Schmidt, Nucl. Phys. **A 531** (1991) 709.

[5] H. L. Ravn, P. Bricault, G. Ciavola, P. Drumm, B. Fogelberg, E. Hagebo, M. Huyse, R. Kirchner, W. Mittig, A. Mueller, H. Nifenecker, E. Roeckl, Nucl. Instrum. Methods **B 88** (1994) 441.

Properties of light nuclides produced in the fragmentation of ^{238}U

M. V. Ricciardi[(1)], K. -H. Schmidt[(1)], P. Armbruster[(1)], J. Benlliure[(2)], M. Bernas[(3)], T. Enqvist[(1)], F. Rejmund[(1)]

(1) GSI – Planckstr. 1 – 64291 Darmstadt - Germany
(2) Univ. Santiago de Compostella – E-15706 Santiago de Compostella - Spain
(3) IPN Orsay – IN2P3, F-91406 Orsay - France

In the last years, motivated by the plans for the construction of ADS and RIB facilities, fragmentation and fission reactions at intermediate energies have acquired a greater interest. The physics of such reactions is still a subject of research, and precise experimental data are needed to test the reliability of the theoretical estimations.

Experiments on the formation of residual nuclei from ^{238}U, ^{208}Pb, ^{197}Au, and ^{56}Fe beams on several targets at relativistic energies have already been performed in inverse kinematics with the fragment separator (FRS) at GSI [1]. Some attractive peculiarities of the in-flight separation are that radioactive fragments can be measured before they decay, the whole isotopic distribution can be obtained for every element, and, once the isotopes are identified, their velocities can precisely be evaluated from their magnetic rigidities. This method yields absolute and extremely accurate velocity values. Here, we will present the result of our investigations on the light residues produced in the fragmentation of 1·A GeV ^{238}U + Ti, and we will compare our preliminary results to previous knowledge.

An important result concerns the velocities of these residues. Morissey [2] showed that the average longitudinal momentum transfer for residual nuclei with masses close to the mass of the mother nucleus ($\Delta A < 50$) increases linearly with the mass loss ΔA. Although the validity of this systematic dependence on ΔA could not be proved for large mass loss due to the uncertainties of the measurements, it seemed reasonable to expect that a more violent collision will produce a larger momentum transfer. On the contrary, Lindenstruth [3], analysing the residual nuclei produced in the interaction of gold with several targets, showed that for $\Delta A > 70$ the momentum transfer stops definitely to increase and eventually starts slowly to decrease. In the present experiments, the velocities of the reaction products could be determined with high precision, and this allows us to check the finding of Lindenstruth. In figure 1 (left) the mean values of the velocity-spectra of fragmentation residues are collected for several elements. Our preliminary data (●) are compared with those obtained in the reaction 1·A GeV ^{238}U + Pb [7] (●), where the acceleration of light elements is even more enhanced. Our results confirm the finding of Lindenstruth in the sense that the momentum transfer does not increase further when the mass loss becomes very important. In addition, we find a clear inversion of the trend for the very light products which are found to be even slightly faster than the projectiles. The reason for this acceleration is not obvious. A possible explanation could be the interaction between the surviving part of the projectile and the expanding fire streak behind it in the later stage of the collision. Another interesting peculiarity of the fragmentation of ^{238}U is the mean N/Z of the produced elements. In figure 1 (right) the EPAX systematics [4] for a ^{197}Au projectile (---) and the stability line are reported (—). These two reference lines are compared with several experimental data. Results from the reactions 800·A MeV ^{197}Au + p [5] (☐) and 414·A MeV ^{56}Fe + p

[6] (△) follow the EPAX systematics. In these cases, the produced fragments are not far from the mother nucleus. However the reactions 1·A GeV ^{238}U + Pb [7] (●), 750·A MeV ^{238}U + Pb [8] (●) and 1·A GeV ^{238}U + Ti (our data) (●) leave the EPAX evaporation corridor, and the more the produced light-nuclides are far from the mother nucleus, the more neutron-rich they are, up to the point that they even cross the stability line. A possible explanation could be found in the predictions of statistical multi-fragmentation models (see [9]). In these models, the light products emerge from the freeze-out of a low-density configuration. Since most of the excitation energy was spent for the disintegration of the system, their secondary deexcitation starts from rather low temperature. Thus these products have larger N/Z-ratios than the fragments produced as a result of evaporation from the mother nucleus.

Properties of light projectile fragments from collisions of massive nuclei have been measured with a high-precision spectrometer. Unexpectedly high velocities and deviations of the N/Z ratio from the evaporation corridor have been found. While the N/Z ratio seems to scale with the mass loss, the velocities also strongly depend on the target nucleus. These features, which seem to be related to multifragmentation, give important information on the dynamics of relativistic nuclear collision.
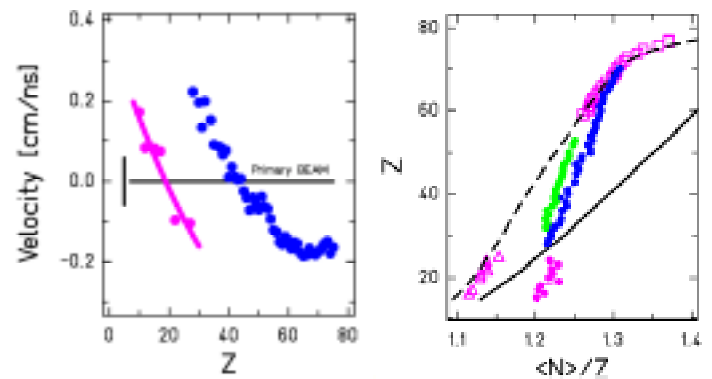

Figure 1: Left: Mean velocities of the fragmentation residues (see text for symbols). Right: Mean N/Z-ratio of the isotopic distributions of the produced elements (see text for symbols).

[1] http://www-wnt.gsi.de/kschmidt/activiti.htm

[2] D. J. Morrissey, *Phys. Rev.* **C 39** (1989) 460

[3] V. Lindenstruth, *GSI-93-18* (1993)

[4] K. Sümmer, B. Blank, *Phys. Rev.* **C 61** (2000) 034607

[5] F. Rejmund et al., *Nucl. Phys.* **A 683** (2001) 540

[6] W. R. Webber et al., *Astr. Jour.* **508** (1998) 949

[7] T. Enqvist et al., Nucl. Phys. **A 658** (1999) 47

[8] J. Benlliure et al., *Eur. Phys. J.* **A 2** (1998) 193

[9] A. S. Botvina et al., *Nucl. Phys.* **A 531** (1991) 709

Critical analysis of dissipative effects in fission

B. Jurado, A. Heinz, A. Junghans, K.-H. Schmidt, GSI Darmstadt, Germany

J. Benlliure, Univ. Santiago de Compostela, Spain

T. Enqvist, Univ. Jyväskylä, Finland

F. Rejmund, IPN Orsay, France

According to Grangé and Weidenmüller [1], dissipation effects in the fission process of a hot heavy-nucleus lead to a time-dependent fission-decay width Γ_f (t) that is first suppressed, then increases gradually and finally reaches a stationary value Γ_{stat}. see full line in figure 1.
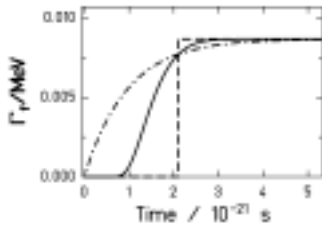
Figure 1: $\Gamma_f(t)$ obtained from the solution of the Fokker-Planck eq. [2] (full line) in comparison with two approximations. The dashed-dotted line corresponds to the approximation (a) and the dashed line to the approximation (b)

However, the implementation of this function in a nuclear-reaction code is rather complicated, and thus most codes use one of the following approximations: (a) an exponential in-grow function of the form $\Gamma_f(t) = \Gamma_{stat}(1 - \exp(-2.3 \cdot t / \tau_f))$ and (b) a step function that switches from zero to the stationary value Γ_{stat} at the transient time τ_f, where the Fokker-Planck solution raises up to 90% of its stationary value. Both approximations are depicted in figure 1. Compared to the exact solution, the description (a) overestimates the fission width, while description (b) underestimates the fission width up to the transient time. We implemented both approximations in our Abrasion-Ablation Monte-Carlo code ABRABLA [3].
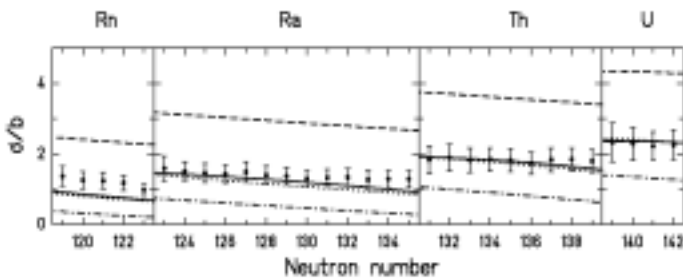

Figure 2: Experimental total nuclear-induced fission cross sections (black dots) as a function of the neutron number for different Rn, Ra, Th and U isotopes at 420 A MeV on a lead target. The data are compared with four calculations, see text

Model calculations are compared to measured total nuclear fission cross sections of different projectiles in figure 2. The full line represents a calculation with the description (b) and a value of the dissipation coefficient, $\beta = 2 \cdot 10^{21} s^{-1}$. This combination shows a very good agreement with the data. However, the combination $\beta = 2 \cdot 10^{21} s^{-1}$ and description (a) clearly overestimates the cross sections, dashed line in figure 2. Nevertheless, the reproduction of the total fission cross sections with description (a) is also possible if we increase the transient time by increasing β up to $9 \cdot 10^{21} s^{-1}$, this is represented in figure 2 by the dotted line. The dashed-dotted line shows that the combination $\Gamma_f(t)$ according to (b) and $\beta = 9 \cdot 10^{21} s^{-1}$ underestimates the cross sections.

The experiment also allowed to determine the nuclear charges of the fission fragments. In figure 3 we compare the two combinations of β and $\Gamma_f(t)$ that reproduce the total fission cross sections of figure 2 with experimental partial fission cross sections. We observe that only the step-function with $\beta = 2 \cdot 10^{21} s^{-1}$ fits the data, while description (b) leads to important deviations from the data.
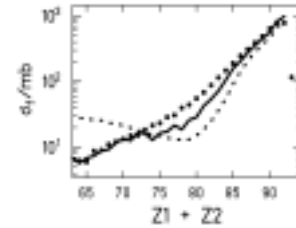

Figure 3: Fission cross sections for ^{238}U on CH_2 at 1 A GeV (full dots) as a function of the sum of the charges of the two fission fragments. The data are shown in comparison with two calculations. The full line is a calculation done with description (b) and $\beta = 2 \cdot 10^{21} s^{-1}$, and the dotted line is a calculation with description (a) and $\beta = 9 \cdot 10^{21} s^{-1}$

Our analysis is based on both a new experimental information from fission induced by relativistic nuclear collisions and the implementation of different in-grow functions in the same code. We conclude that the deduced dissipation coefficient β depends strongly on the function which is used to describe $\Gamma_f(t)$. We have found that all our data are well reproduced with a step function for $\Gamma_f(t)$ (option (b)) and $\beta = 2 \cdot 10^{21} s^{-1}$ and that the most widely used description of $\Gamma_f(t)$, an exponential in-grow function, does not reproduce our data, because it fails to describe the essential feature of the solution of the Fokker-Planck equation, namely the practically complete suppression of fission during most part of the transient time. Our result sheds severe doubts on part of the previous work on nuclear dissipation.

References

1 P. Grangé et al., Phys. Rev. C 27 (1983) 2063

2 S. Chandrasekhar, Rev. Mod. Phys. 15 (1943) 1

3 A. Heinz et al., GSI Ann. Rep.(1999)30 and references within

Quaternary Fission of ^{252}Cf ^{B,G}

Yu.N. Kopatch[1], M. Mutterer[2], J. von Kalben[2], H.-J. Wollersheim[1], E. Lubkiewicz[3], and P. Adrich[3]

[1] *GSI Darmstadt*, [2] *TU Darmstadt*, [3] *Cracow University, Poland*

The rare ternary fission process ($\simeq 1/260$ relative to binary fission, for ^{252}Cf) is of particular interest not only for the understanding of the fission process itself, but also as a source of various neutron-rich light nuclei [1]. The study of "exotic" light nuclei is a major topic in modern nuclear structure physics with radioactive beams. The even rarer quaternary fission (QF) mode [2], when two light charged particles (LCP) are emitted simultaneously in addition to the main fission fragments, can originate either from a break-up of unstable species among the LCPs, e.g. ^{7}Li*, ^{8}Be, ^{9}Be* ("pseudo" quaternary fission), or from the independent emission of two LCPs ("true" quaternary fission).

The QF processes were studied at GSI using a spontaneous ^{252}Cf fission source (~ 5000 fissions/sec). The LCPs were identified by a set of eight ΔE-E telescopes (12 μm + 380 μm Si detectors of 1 cm^2 each) subtending a total solid angle of $\sim 20\%$. Fission fragments and the 6.1 MeV α-particles from the ^{252}Cf radioactivity were stopped in suitable absorbers placed between source and detectors. The telescopes allowed for a clean separation of the LCP nuclear charges. A total of 255 α-α coincidences were detected, within a time window of 10 nsec. Simultaneously, single LCP events with the emission of ternary α, Li and Be particles were registered and could be used as a reference.
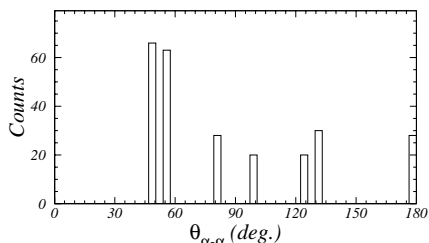

Figure 1: Measured relative angles for α-α coincidences.

Figure 1 shows the number of α-α coincidences as a function of the relative angle between the centers of the telescope surfaces. There is a clear enhancement of the quaternary fission yield at the smaller angles which is attributed to the break-up of ^8Be LCPs, while the homogeneous distribution at the larger angles signals the true QF events. Simple estimates based on the kinematics of the ternary ^{8}Be decay in flight show that the largest possible angle between the two α-particles from the ^{8}Be ground-state decay ($T_{1/2} = 0.07$ fs, $Q = 0.092$ MeV) equals 8°, while the smallest distance between neighbouring telescopes corresponds to an opening angle of 16°. Thus, the observed enhancement in the angular distribution is presumably due to the decay from the first excited level in ^{8}Be ($T_{1/2} = 3 \times 10^{-22}$ s, $Q = 3.13$ MeV). In that case the distribution of the relative angles is expected to be significantly broader [2].

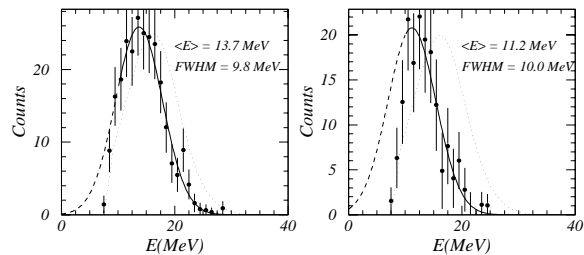The energy spectra of the true and pseudo QF components are presented in Fig. 2. The yield for the true

Figure 2: Energy spectra (corrected for the energy loss in the absorbers) of the true quaternary α-particles (left) and α-particles mediated by ^{8}Be* LCPs (right). The solid lines are Gaussian fits, the dotted line is the measured ternary α-particle spectrum ($< E >= 15.9$ MeV).

α-α QF, assuming isotropic distribution of the relative angles, is estimated as $(3 \pm 1) \times 10^{-4}$ relative to the yield of ternary ^{4}He. The two quaternary α-particles mediated by the ground-state decay of ^{8}Be are registered in our set-up as an admixture to the Li spectrum, as they fall into the same range in the ΔE-E patterns. An attempt was made to disentangle these two contributions by fitting the known Li energy spectrum [3] and the sum spectrum of the two α-particles from the ^{8}Be decay, considering the energy loss in the absorbers and ΔE detectors, to the measured E_{rest} spectrum (Fig. 3).
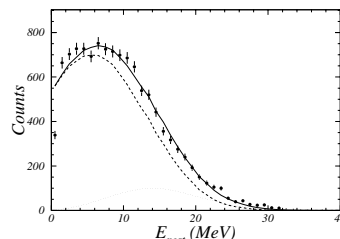

Figure 3: Decomposition of the E_{rest} spectrum gated on the ΔE-E patterns for Li (points): Dashed line - ternary Li spectrum, dotted line - sum spectrum of two α's hitting a telescope, solid line - sum of both components.

The result (still preliminary) for the ^{8}Be ground-state yield is $\simeq 1 \times 10^{-3}$ relative to the yield of ternary ^{4}He. The systematic error in this procedure is fairly large ($\geq 50\%$), because of the uncertainty in the energy loss corrections and the not precisely known ternary Li spectrum. In a forthcoming experiment it is thus planned to separate the Li ternary particles unambiguously from the double α-particle hits in each telescope by applying pulse-shape discrimination in suitable E_{rest} detectors.

References

[1] M. Mutterer *et al.*, Proc. 2nd Int. Conf. on Fission and Properties of Neutron-Rich Nuclei, St.Andrews, 1999, (World Scientific) (2000), p. 316.

[2] F. Gönnenwein *et al.*, Proc. Int. Workshop Fission Dynamics of Atomic Clusters and Nuclei, Luso, 2000, (World Scientific), in press.

[3] P. Singer, Dissertation, TU Darmstadt (1996).

Mean field and beyond in α-decay chains of superheavy elements[B+G]

P.–G. Reinhard[1], P. Fleischer[1], M. Bender[2],

[1] Institut für Theoretische Physik, Universität Erlangen, Staudtstr. 7, D–91058 Erlangen
[2] Gesellschaft für Schwerionenforschung, Planckstr. 1, D–64291 Darmstadt

Recent experiments at GSI [1] and JINIR Dubna [2] brought evidence for the synthesis of new superheavy elements. One of the key observable in these experiments is the Q_α value along the α-decay chains. In this contribution, we want to investigate this observable within self-consistent mean-field models.

We consider two different models, the Skyrme-Hartree-Fock approach (SHF) and the relativistic mean-field model (RMF), for a most recent review see [3]. From the world of different parametrisations we confine the discussion to a few well adjusted, typical and recent sets. For SHF we consider the parametrisations SkP, SkI3, SkI4, and SLy6. The force SkP uses effective mass $m^*/m = 1$ and is designed to allow a self-consistent treatment of pairing. The other forces all have smaller effective masses around $m^*/m = 0.7 - 0.8$. The force SLy6 stem from an attempt to cover properties of pure neutron matter together with normal nuclear ground-state properties. The forces SkI3/4 employ a spin-orbit force with isovector freedom to simulate the relativistic spin-orbit structure. SkI3 contains a fixed isovector part exactly analogous to the RMF, whereas SkI4 is adjusted allowing free variation of the isovector spin-orbit force. The modified spin-orbit force has a strong effect on the spectral distribution in heavy nuclei and thus for the predictions of superheavy elements. For the RMF we consider the parametrisations NL-Z2 and NL3. The force NL-Z2 comes from fits much similar to those of SkI3 and SkI4. NL3 is fitted without looking at the electron-scattering formfactor but with taking more care about the isovector trends. We ought to remind here that these different parametrisations produce much different predictions for the magic shell closure in SHE [4, 5].

Fig. 1 compares calculated and experimental α energies for the new isotopes. Most models make similar predictions at the lower end of the chains and these agree very nicely with the available new data for both chains. Larger differences among the forces show up when going to heavier systems. This is mainly due to differently pronounced shell closures which produce these curious kinks. Having a closer look on the deformation energies shows that one comes into a regime of very soft nuclei with pronounced shape isomerism. The mean-field state represents the one configuration at the absolute minimum of energy. But many other configurations are energetically competitive in soft nuclei. Thus one needs to consider a correlated ground state built from an appropriate coherent mixture of configurations. In practice, we superpose the states along the quadrupole deformation path using the generator-coordinate method [6]. The effect of such correlations is shown in Fig. 2. They wipe out the kinks and produce a smooth trend throughout. There is little correlation effect at the lower end of the chain such that the orginally given good agreement with data is maintained. Moreover, correlations bring the predictions from the the various forces closer together again. The then remaining difference is a clear signal of different bulk properties deep within the models, yet to be worked out in detail.

To conclude, mean-field models provide a pertinent description for the Q_α values along the recently measured decay chains of superheavy elements. Correlations effects beyond mean field need to be taken into account for the heavier isotopes.

References

[1] S. Hofmann *et al.*, GSI preprint 2000–52.
[2] Yu. Oganessian *et al.*, Phys. Rev. C **62**, 41604 (2000).
[3] P.-G. Reinhard *et al.*, Comm. Nucl. Part. Sci. (2001).
[4] K. Rutz *et al.*, Phys. Rev. C **56**, 238 (1997).
[5] M. Bender *et al.*, Phys. Rev. C **60**, 034304 (1999).
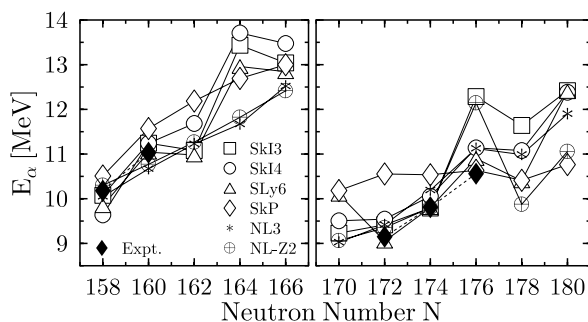[6] P.–G. Reinhard, *et al.*, RIKEN Review **26**, 23 (2000)

Figure 1: Ground-state-to-ground-state α energies for the α-decay chains containing $^{270}_{160}110$ (left panel) and $^{282}_{176}116$ (right panel) from mean-field calculations with the forces as indicated. Filled diamonds denote the experimental values.
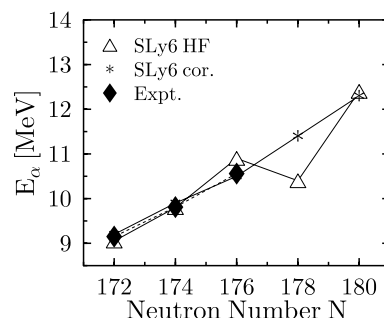

Figure 2: Ground-state-to-ground-state α energies for the decay chain containing $^{282}_{176}116$ computed with the force SLy6. Compared are calculations with and without taking ground-state correlations into account.

Shell stabilization in superheavy elements[B+G]

M. Bender,[1] P.–G. Reinhard[2]

[1] Gesellschaft für Schwerionenforschung, Planckstr. 1, D–64291 Darmstadt
[2] Institut für Theoretische Physik, Universität Erlangen, Staudtstr. 7, D–91058 Erlangen

Superheavy elements (SHE) are by definition those very heavy nuclei which have a negligible liquid-drop fission barrier. Quantum mechanical shell effects create one or several minima in the potential energy surface which stabilize the nucleus against fission. This additional binding from shell effects is quantified by the shell correction energy which is thus a first hint on the fission stability.

The shell correction energy can be computed by comparing the actual discrete distribution of single-particle energies with a smoothened level density. The weakly–bound SHE require a careful treatment of the continuum which we perform according to the recipe of [1]. Fig. 1 shows the shell correction energies from fully self-consistent calculations with the Skyrme interactions SkI3 and SLy6 and the relativistic mean-field interactions NL3 and NL–Z2. Remind that the shell correction is always sharply peaked at shell closures for nuclei up to Pb. This changes when going to SHE. There emerges a broad island of shell stabilization which spreads around the shell closures predicted by the various forces. Similar pattern are found in macroscopic-microscopic models. As a consequence, the significant differences seen in the prediction of magic numbers when looking at the δ_{2q} [2] are much mellowed by the generally softer pattern of the shell energy which looks similar for all models investigated in [3]. The reason for this behaviour is an accumulation of states with low angular momentum at the Fermi surface for these SHE. On one hand, this causes the fast changes of the various shell closures by small shifts of individual levels [4]. On the other hand, this turns the shell effect of individual levels into the shell effect of a bunch of levels more independent on the subtle details of actual shell closures.

Spherical shell corrections are, of course, a first indicator only for the stability of SHE. What finally counts is the fission barrier. And fission can go unusual paths in SHE.
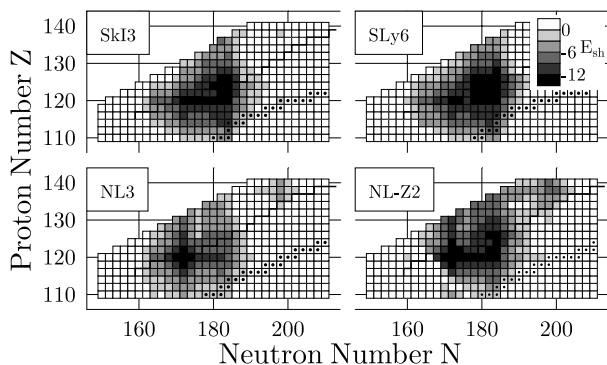

Figure 1: Total shell correction for spherical configurations of superheavy nuclei extracted from self–consistent calculations with the effective interactions as indicated. The (calculated) two–proton drip line and the valley of stability are emphasized. Data taken from [3].
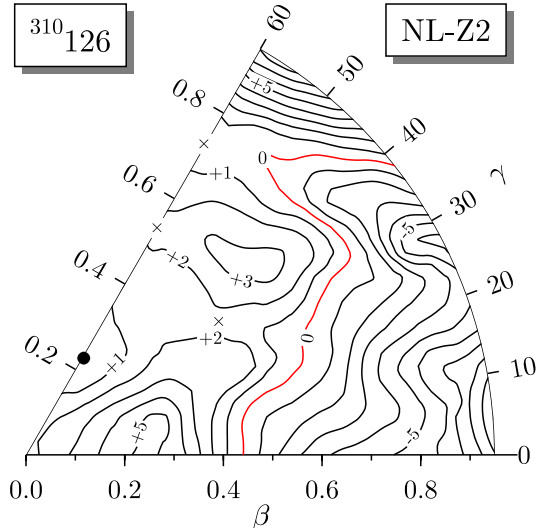

Figure 2: Potential energy surface of $^{310}_{184}126$ in the β–γ plane calculated with the relativistic mean-field interaction NL–Z2. The filled circle denotes the oblate minimum, while crosses denote the various saddle points. Deformation energies in MeV are with respect to the oblate ground state.

Fig. 2 shows as an example the potential energy landscape of $^{310}_{184}126$ in the full triaxial plane. In spite of the huge shell correction of more than -12 MeV at spherical shape the actual ground state of $^{310}_{184}126$ is oblate when calculated with NL–Z2. Triaxial configurations reduce the axial prolate barrier of more than 5 MeV to 1.8 MeV. The result has to be taken with precaution because these detailed fission pattern seem to depend sensitively on the actual nucleus and force used. $^{292}_{172}120$ has spherical shape and a triaxial barrier of nearly 6 MeV when calculated with the same force. Skyrme interactions give a similar potential landscape in $^{310}_{184}126$ but with a spherical ground state and substantially higher barriers around 9 MeV, see [5]. This systematic difference in fission barrier heights when comparing Skyrme interactions and relativistic mean field has already been seen in [6] and still needs to be understood. Fig. 2 demonstrates, however, that one has to be aware of surprises in this region of nuclei and that there is still a bulk of work ahead to uncover all these features.

References

[1] A. T. Kruppa et al., Phys. Rev. C **61**, 034313 (2000).
[2] K. Rutz et al., Phys. Rev. C **56**, 238 (1997).
[3] M. Bender, W. Nazarewicz, P.–G. Reinhard, in preparation.
[4] M. Bender et al., Phys. Rev. C **60**, 034304 (1999).
[5] S. Ćwiok et al., Nucl. Phys. **A611**, 211 (1996).
[6] M. Bender et al., Phys. Rev. C **58**, 2126 (1998).

Proton shell closures in proton–rich heavy nuclei

T. Cornelius[1], M. Bender[2], T. Bürvenich[1], L. Kudling[1], A. Sulaksono[1],
P.–G. Reinhard[3], J. A. Maruhn[1], W. Greiner[1]

[1] Institut für Theoretische Physik, Universität Frankfurt, Robert-Mayer-Str. 8–10, D–60325 Frankfurt am Main
[2] Gesellschaft für Schwerionenforschung, Planckstr. 1, D–64291 Darmstadt
[3] Institut für Theoretische Physik, Universität Erlangen, Staudtstr. 7, D–91058 Erlangen

Magic numbers are a key feature of any finite Fermion system as they provide crucial clues on the underlying mean field. The study of shell closures is thus very interesting in exotic nuclei. One wants to know how the shell closures develop when moving towards the driplines. It is now well–established for neutron–rich $N=20$ and $N=28$ isotones that the neutron shells fade away. This gives rise to a transient regime of pronounced low-lying collecive states and finally to stable ground-state deformation [1]. There are hints from the systematics of 2^+ and 4^+ excitation energies in Cd and Pd isotopes that also the $N=50$ and $N=82$ shells are weakened when going towards neutron–rich nuclei [2]. All these examples concern a weakening of neutron shells. The situation seems to be different for protons. For light nuclei there is no indication that the proton shell closures fade away towards the proton drip line. But the analysis of recent mass measurements [3] shows a substantial weakening of the two–proton shell gap

$$\delta_{2p}(Z,N) = E(Z-2,N) - 2E(Z,N) + E(Z+2,N)$$

for very proton-rich Pb isotopes. It is speculated whether this is related to a weakening of the $Z=82$ shell [4]. This contribution looks at this problem from a theoretical perspective.

As tool we take self-consistent mean-field models which are nowadays well developed and provide a pertinent picture of the nuclear properties throughout the whole mass table. We consider two different models, the Skyrme-Hartree-Fock approach (SHF) and the relativistic mean-field model (RMF). We take one typical parametrisation for each model, SkI3 for the SHF and NL3 for the RMF, see e.g. [5]. SHF as well as RMF produce single–proton spectra in Pb with a well developed magic gap at $Z=82$ for all isotopes up to the dripline. This is confirmed by the systematics of the shell-correction energies extracted from self-consistent calculations [6]. The δ_{2p} are presented in Fig. 1. The upper panel shows δ_{2p} for spherical calculations in Pb as well as in its $Z\pm2$ neighbours Po and Hg. The theoretical results give an almost constantly large δ_{2p} along the whole isotopic chain, in compliance with the large spectral gap and shell-correction energy. But the results for δ_{2p} are clearly at variance with the data. This changes dramatically when allowing for ground–state deformation, see the lower panel. While the ground states of Pb isotopes stay spherical, the ground states of proton-rich Hg and Po isotopes become deformed. They thus gain energy which significantly reduces the extremely sensitive double difference δ_{2p}. The findings are consistent with the currently available data which confirm deformation softness in these heavy proton-rich isotopes, see e.g. [7] and references therein. Important for our purpose is: (i) $^{180-190}$Hg have oblate deformed ground states, (ii) data on excitation spectra and charge radii for Pb isotopes are consistent with spherical ground states, and (iii) proton-rich Po isotopes show an increased collectivity.

In summary the observed weakening of δ_{2p} around $Z=82$ is caused by the increased collectivity of the Hg and Po isotopes, and not by a quenching of the $Z=82$ shell. Large values of δ_{2p} are a sufficient, but not a necessary indicator for a shell closure. This example shows that a thorough analysis of magic shells requires a simultanous consideration of various signals, e.g. the δ_{2p} together with energy and strength of low-lying 2^+ and 4^+ states, possibly complemented by α-decay hindrance factors [8]. True proton-shell quenching, however, is expected for the next magic proton number in the realm of superheavy elements [9].
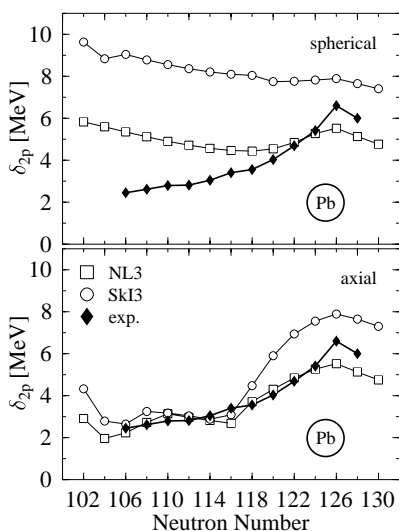
References

[1] S. Pèru et al., Eur. Phys. J. **A9**, 35 (2000).
[2] T. Kautzsch et al., Eur. Phys. J. **A9**, 201 (2000).
[3] T. Radon et al., Nucl. Phys. **A677**, 75 (2000).
[4] Yu. N. Novikov et al., submitted to Nucl. Phys. A.
[5] P.–G. Reinhard et al., Comm. Nuc. Part. Sci. (2001)
[6] M. Bender et al., in preparation.
[7] K. Heyde et al., Phys. Rev. **C53**, 1035 (1996).
[8] J. Wauters et al,, Phys. Rev. Lett. **72**, 1329 (1994).
[9] M. Bender et al., Phys. Rev. C **60**, 034304 (1999).

Figure 1: Two–proton shell gap δ_{2p} for Pb isotopes calculated with SHF (force SkI3) and RMF (force NL3) and compared with experimental data. Upper panel: from spherical configurations of all nuclei. Lower panel: allowing for ground-state deformations.

Microscopic Description of Charge and Matter Distributions of Long-Tailed and Halo Nuclei

M. Tomaselli[a,b], T. Kühl[b,c], P. Egelhof[b,c], C. Kozhuharov[b], D. Marx[b], A. Dax[b],
S.R. Neumaier[b], W. Nörtershäuser[b,d], M. Mutterer[a], H. Wang[b,e], H.-J. Kluge[b], and S. Fritzsche[f]

[a] Darmstadt University, [b] GSI Darmstadt, [c] Mainz University, [d] Tübingen University,
[e] Tokyo University, [f] Kassel University

Elastic proton-scattering experiments in inverse kinematics recently performed at GSI [1] have reopened important, partially unresolved questions concerning the physics of the halo nucleus ^{11}Li. In order to obtain a deeper insight into the halo structure of light exotic nuclei and to understand the difference between the matter and the charge distributions, microscopic calculations for the ground states of the ^{6,7,9,11}Li and ^{7,9}Be isotopes have been performed within the Dynamic-Correlation Model (DCM) [2].

The DCM describes the ground states of nuclei in terms of interacting clusters: valence particles and intrinsic vacuum states. The amplitudes of the mixed-mode wave-functions are derived in the framework of non-perturbative solutions of the Equation of Motion. Theoretically, the model spaces for the ground states of the ^{6,7,9,11}Li and the ^{7,9}Be isotopes are constructed by allowing valence particles to be scattered to higher configuration states ($2\,\hbar\omega$) and to interact with the core intrinsic states formed by exciting particles from the s, p-shell. The single-particle states used as input in the DCM have been approximated by harmonic oscillators with a state-dependent range introduced to reproduce the single-particle radii as calculated in a Wood-Saxon potential well. The single-particle energies are also obtained in this procedure. The two-body matrix elements are the same as used in Ref. [2].

The matter and charge distributions calculated with this microscopic approach can be used to predict experimentally accessible quantities. In this report we present and discuss the matter distributions for the lithium isotopes ^{7,9,11}Li. Root-mean-square matter and charge radii obtained for the above mentioned beryllium isotopes are also given.

The DCM matter distributions for the lithium isotopes are presented in Fig. 1. The oscillations in the theoretical matter distribution result from the interferences of the

valence and the intrinsic states. For ^{11}Li two matter distributions are shown. The dotted line has been obtained by taking the three neutrons in the p-shell into account, while the solid line considers the effect of the neutons moving in the p, s, and d shells and interacting with the vacuum states. It is obvious that the s and d neutrons as well as the core excitations have a profound influence on the halo structure [4]. While there are experimental values for the matter radii of all accessible lithium and beryllium isotopes [5], the charge radii are only known for the stable isotopes [5, 6]. Experimental and theoretical values are in good agreement. However, for a better understanding of the neutron halos influence on the core nucleus, it is desirable to determine the charge radii of the radioactive lithium isotopes experimentally, particularly for ^{11}Li. For this purpose an experiment is being prepared at GSI and ISOLDE, CERN [7] to determine this value by means of an optical isotope-shift measurement. The agreement of the calculated (rms) charge and matter radii for the lithium isotopes with experimental data [5] is good in all cases with the exception of the matter radius of ^{11}Li, which is considerably larger than the experimental value. For ^{7}Be and ^{9}Be the calculated radii (Tab.1) are close to the values of Ref. [5]. It should be mentioned that the experimental values for the matter distribution are model-dependent and that new proton-scattering data from GSI [3] indicate a larger matter radius than the one given previously in Ref. [5]. The matter distribution of ^{11}Li (solid line) and the calculated matter radius of 3.64 fm agree with the phenomenological distribution and with the radius of 3.65 fm given in Ref. [3].

Table 1: Rms-mass and -charge radii for beryllium isotopes

	$R_{matter}^{calc.}$	$R_{charge}^{calc.}$	$R_{matter}^{exp.}$ [5]	$R_{charge}^{exp.}$ [5]
^{7}Be	2.38 fm	2.39 fm	2.31(2) fm	? fm
^{9}Be	2.46 fm	2.62 fm	2.38(1) fm	2.47(1) fm

References

[1] S.R. Neumaier et al., submitted to Nucl. Phys. A (2001); G.D. Alkhazov et al., Phys. Rev. Lett. 78, 2313 (1997)

[2] M. Tomaselli et al., APAC 1999, Hyperfine Interactions 127, 95 (2000); Phys. Rev. C62 (2000), 67305

[3] A.V. Dobrowolsky et al., GSI Report (1999) and Verhdlg. DPG 35, 5 (2000)

[4] M. Tomaselli, C. Kozhuharov, and T. Kühl, 2001 in preparation

[5] I. Tanihata et al., Phys. Lett. B 206, 592 (1988)

[6] C.W. de Jaeger et al., At. Data, Nucl. Data Tables 14, 479 (1974)

[7] A. Dax et al., CERN/INTC 2000-006 INTC/P118

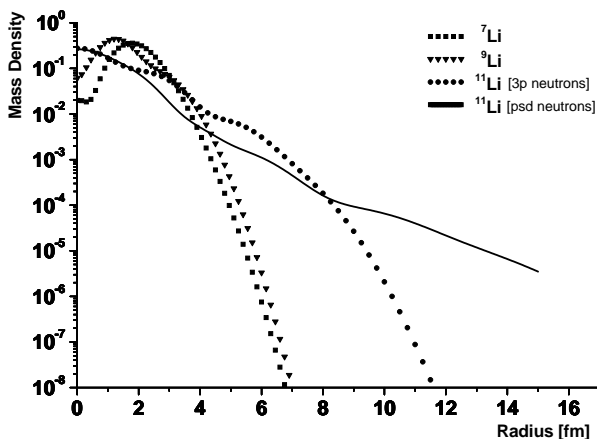Fig. 1: Calculated mass distribution for ^{7,9,11}Li. The halo structure of ^{11}Li is mainly associated to sd neutrons and to core excitations.

Ground-State Structure based on Realistic NN-Potentials

H. Feldmeier, P. Krafft, T. Neff and R. Roth (GSI)

A long standing goal of theoretical nuclear physics is the description of nuclear structure starting from a realistic nucleon-nucleon potential. All realistic NN-interactions show however two characteristics that inhibit a treatment of the many-body problem in a mean-field model. Firstly, the local part of the interaction shows a strong short-range repulsion (the so called *core*) and, secondly, there is a strong tensor part. Both properties give rise to special correlations in the many-body state, which cannot be described by Slater determinants or a superposition of shell model states from a few major shells.

In the framework of the Unitary Correlation Operator Method (UCOM) [1] we describe both types of correlations explicitly by unitary transformations of shell model type many-body states. Thus we obtain states that contain the relevant correlations induced by the interaction between the nucleons.

To describe the short-range correlations caused by the repulsive core of the interaction the unitary correlation operator generates a radial distance-dependent shift in the relative coordinate of each pair of particles. By that the particles are shifted out of the repulsive region of the interaction. Alternatively the correlation operator can be used to transform the Hamilton operator with the bare interaction.

For the correlations induced by the tensor part of the interaction a similar procedure is applied. The new aspect is that tensor interactions correlate coordinate and spin space in a complex way. The unitary transformation, which describes these correlations, acts on the angular part of the relative coordinates in dependence on the spin orientation of the two particles.

As a preliminary step towards a full ab initio calculation on the basis of the central and tensor correlated Bonn-A potential [2] we use a parameterized correction to account for tensor correlations. The core-induced central correlations are fully included by a spin- and isospin-dependent correlation operator [1]. In order to account for tensor correlations we add to the Bonn-A potential a correction in the $S = 1, T = 0$ channel. According to the structure expected for the tensor correlated interaction the correction consists of an additional attractive central potential and a repulsive momentum-dependent part. Three parameters (strength of local correction, and strength and range of momentum part) are adjusted to reproduce the experimental binding energies and charge radii of ^{4}He, ^{16}O, and ^{40}Ca.

Based on this correlated Bonn-A potential the many-body problem is treated in the framework of Fermionic Molecular Dynamics (FMD) [3]. The uncorrelated many-body state is described by a Slater determinant of gaussian one-body states, which contain the mean position, mean momentum, complex width and spin orientation as variational parameters. The ground-state wave function is determined by energy minimization with the correlated interaction.

The Figure shows the ground state one-body density distributions of ^{16}O, ^{20}Ne, and ^{24}Mg obtained with this method. For ^{16}O we find a spherical shell-model like distribution with a characteristic depletion of the central density. ^{20}Ne shows a prolate axially symmetric density distribution with α-like structures at the ends and a toroidal distribution in the central plane. Finally ^{24}Mg exhibits a complicated triaxial deformation with some remnants of α-clustering.

These calculations demonstrate the flexibility of the FMD basis as well as the possibility to perform nuclear structure calculations based on realistic NN-interactions in a nearly ab initio way. Our next step will be the inclusion of tensor correlations in a stringent way by calculating the appropriate unitary correlation operator explicitly.

[1] H. Feldmeier, T. Neff, R. Roth, J. Schnack; Nucl Phys. A632 (1998) 61.

[2] R. Machleidt; Adv. Nucl. Phys. 19 (1989) 189.

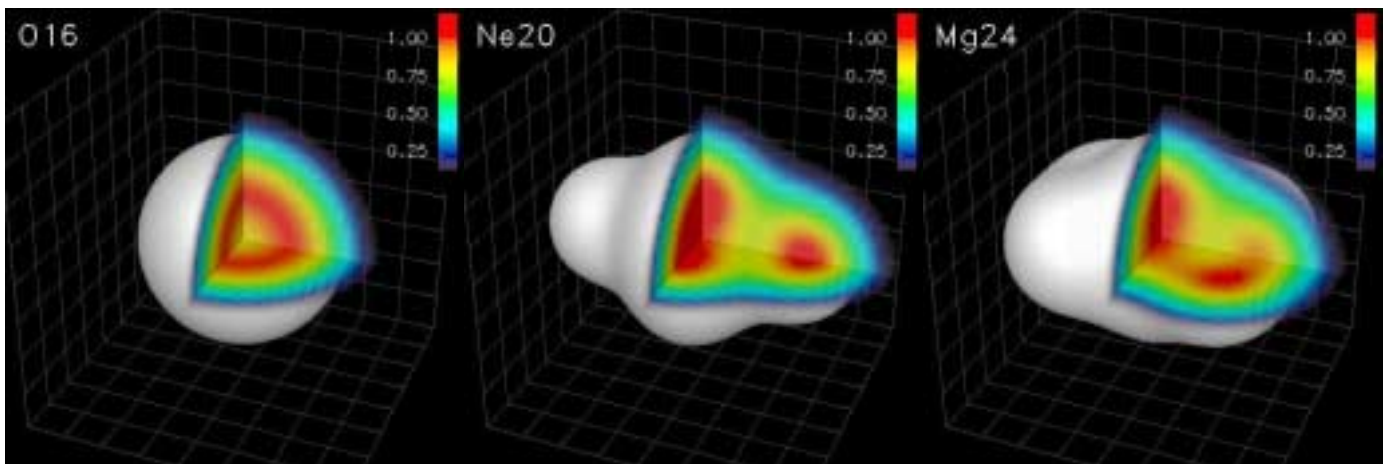[3] H. Feldmeier, J. Schnack; Rev. Mod. Phys. 72 (2000) 655.

Figure 1: One-body density distributions (3-dimensional) of ^{16}O, ^{20}Ne, and ^{24}Mg. The white body shows the iso-density surface corresponding to half nuclear matter density ($\rho_0 = 0.17$fm^{-3}). The embedded planar cuts show the interior density distribution with color coding according to the color bar (in units of ρ_0). The mesh size of the background grid is 1fm $\times$ 1fm. Visit the FMD-Gallery at http://www.gsi.de/~fmd/.